

# A decade of glaciological and meteorological observations in the Arctic (Werenskioldbreen, Svalbard)

Dariusz Ignatiuk<sup>1</sup>, Małgorzata Błaszczyk<sup>1</sup>, Tomasz Budzik<sup>1</sup>, Mariusz Grabiec<sup>1</sup>, Jacek A. Jania<sup>1</sup>, Marta Kondracka<sup>1</sup>, Michał Łaska<sup>1</sup>, Łukasz Małarzewski<sup>1</sup>, Łukasz Stachnik<sup>2</sup>

<sup>1</sup>University of Silesia in Katowice, Katowice, 40-007, Poland

<sup>2</sup>University of Wrocław, Wrocław, 50-137, Poland

Correspondence to: Dariusz Ignatiuk ([dariusz.ignatiuk@us.edu.pl](mailto:dariusz.ignatiuk@us.edu.pl))

**Abstract.** The warming of the Arctic climate is well documented, but the mechanisms of Arctic amplification are still not fully understood. Thus, monitoring of glaciological and meteorological variables and the environmental response to accelerated climate warming must be continued and developed in Svalbard. Long-term meteorological observations carried out in situ on glaciers in conjunction with glaciological monitoring are rare in the Arctic and significantly expand our knowledge about processes in the polar environment. This study presents the unique important glaciological and meteorological data collected in 2009-2020 in southern Spitsbergen (Werenskioldbreen). The meteorological data are comprised of air temperature, relative humidity, wind speed and direction, shortwave and longwave upwelling and downwelling radiation on 10 minutes, hourly and daily timesealeresolution (2009-2020). The snow dataset includes 49 sampling pointsdata records from 2009-2019 with the snow depth, snow bulk density and SWE (snow water equivalent) data. The glaciological data consist of pointseasonal and annual surface annual winter, summer and netmass balance measurements (point and glacier-wide) for 2009-2020. The paper also includes modelling of the daily glacier surface ablation (2009-2020) based on the presented data. The high-quality and long-term datasets are expected to serve as accurate local forcing data in hydrological and glaciological models and validation of calibration of remote sensing products. The datasets are available from the and Polish Polar Database (<https://ppdb.us.edu.pl/>) and Zenodo (<https://doi.org/10.5281/zenodo.5791748><https://doi.org/10.5281/zenodo.5791748>, Ignatiuk, 2021a; <https://doi.org/10.5281/zenodo.5792168><https://doi.org/10.5281/zenodo.5792168>, Ignatiuk, 2021b).

## 1 Introduction

Long-term meteorological observations carried out in situ on glaciers in conjunction with glaciological monitoring are rare in the Arctic and significantly may be used to expand our knowledge about processes in the polar environment. Terrestrial meteorological monitoring alone does not always adequately address the needs of numerical modelling as well as validation and calibration of numerical models or satellite products regarding glaciers: (Pelliccotti et al., 2014; Gabbi et al., 2017). The warming of the Arctic climate is well documented, but the mechanisms of Arctic amplification are still not fully understood

Definicja stylu: Normalny

Definicja stylu: Nagłówek 2

Definicja stylu: Nagłówek 3

Definicja stylu: Nagłówek 4

Definicja stylu: Bullets: Konspekty numerowane + Poziom: 1 + Styl numeracji: 1, 2, 3, ... + Rozpocznij od: 1 + Wyrównanie: Na lewo + Wyrównanie: 0 cm + Tabulator po: 1,27 cm + Wcięcie: 1,27 cm

Sformatowano: Od tekstu: 0 cm

Sformatowano: Czcionka: + Tekst podstawowy (Times New Roman), 17 pkt, Pogrubienie, Kolor czcionki: Czarny

Sformatowano

Sformatowano

Sformatowano

Sformatowano

Kod pola został zmieniony

Sformatowano

Sformatowano

Sformatowano

Sformatowano

Sformatowano

Sformatowano

Sformatowano

Sformatowano

Sformatowano

Sformatowano

Sformatowano

Sformatowano

Sformatowano

Sformatowano

Sformatowano

Sformatowano

Sformatowano

Sformatowano

Sformatowano

Sformatowano

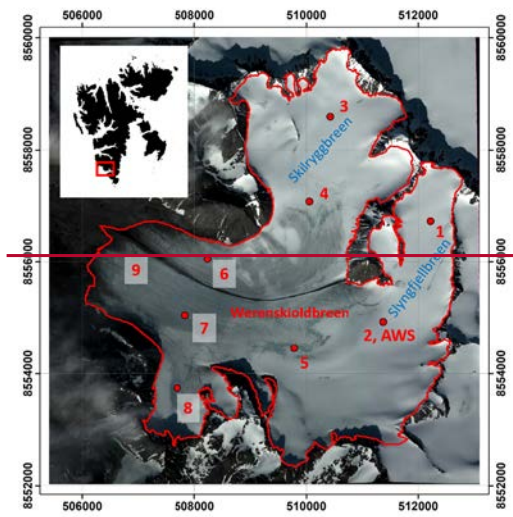
Sformatowano



river gorge. Such a hydrological system allows the glacier basin to be treated as a closed well-defined research laboratory for many hydrological and interdisciplinary studies (Majchrowska et al., 2015; Stachnik et al., 2016b; Lepkowska and Stachnik, 2018; Gwizdała et al., 2018; Stachnik et al., 2019; Osuch et al., 2022). The glacier is situated 15 km to the north from the Polish Polar Station Hornsund. The Stanisław Baranowski Spitsbergen Polar Station (University of Wrocław), a small field station is located at the southern edge of the Werenskiöldbreen terminal moraine. Both facilities greatly simplify the accessibility and logistics of research and monitoring projects.

Sformatowano: Czcionka: + Tekst podstawowy (Times New Roman)

Sformatowano: Czcionka: + Tekst podstawowy (Times New Roman)



Sformatowano: Normalny, Obramowanie: Góra: (Brak obramowania), Dół: (Brak obramowania), Na lewo: (Brak obramowania), Na prawo: (Brak obramowania), Pośrodku: (Brak obramowania), Tabulatory: 7,96 cm, Wyśrodkowany + 15,92 cm, Do prawej

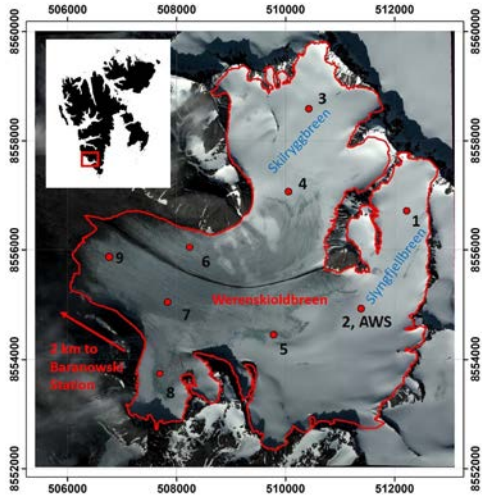


Figure 1: Location of mass-balance stakes (1-9) in 2009-2020 and the automatic weather station (AWS) on Werenskiöldbreen (background: GeoEye, 2010/08/10)

### 3 Instruments and methodology:

#### 3.1 Meteorological monitoring

The automatic weather station (AWS) is located at an altitude of 380 m above sea level (Figure 1), close to the average equilibrium line altitude (ELA) for the years 1959 – 2008 (Noël et al, 2020). The station was installed on the glacier on 15 April 2010. The AWS was mounted on a long steel mast placed in the ice drilling hole (ca. 6 m deep). In the following years, as ablation progressed, the sensors were lowered or the mast was replaced with a new one in close proximity to the original location. The recording of variables (air temperature, humidity, wind speed, shortwave and longwave radiation) has started on 17 April 2010 (Table 1). ~~The CNR4 net radiometer was replaced in 2016 by the CMP3 pyranometers, which resulted in shortwave radiation measurements being continued and longwave radiation measurements being ceased.~~ The Kipp & Zonnen CNR4 consists of two CM3 pyranometers, two CG3 pyrgeometers and temperature sensors (PT100). Pyranometers (180° solid angle) have a glass dome and measure radiation in the range from 300 to 2 800 nm. One of the pyranometers directed upwards measures downwelling radiation, and the second one ~~upwelling which directed downwards~~ measures solar radiation reflected from the earth's surface. ~~(upwelling radiations)~~ Pyrgeometers (180°, 150° solid angle), has silicone windows, which allow radiation measurements in the range from ~~4-5004500 nm~~ to ~~42-00042000 nm~~. Like the pyranometers, the pyrgeometers point

**Sformatowano:** Czcionka: + Tekst podstawowy (Times New Roman), 9 pkt, Pogrubienie, Kolor czcionki: Czarny

**Sformatowano:** Czcionka: + Tekst podstawowy (Times New Roman), 9 pkt, Pogrubienie, Kolor czcionki: Czarny

**Sformatowano:** Normalny, Odstęp Po: 10 pkt, Obramowanie: Góra: (Brak obramowania), Dół: (Brak obramowania), Na lewo: (Brak obramowania), Na prawo: (Brak obramowania), Pośrodkowy: (Brak obramowania)

**Sformatowano:** Czcionka: + Tekst podstawowy (Times New Roman)

**Sformatowano:** Czcionka: + Tekst podstawowy (Times New Roman)

**Sformatowano:** Czcionka: + Tekst podstawowy (Times New Roman), Indeks górny

**Sformatowano:** Czcionka: + Tekst podstawowy (Times New Roman)

**Sformatowano:** Czcionka: + Tekst podstawowy (Times New Roman)

**Sformatowano:** Czcionka: + Tekst podstawowy (Times New Roman)

**Sformatowano:** Czcionka: + Tekst podstawowy (Times New Roman)

**Sformatowano:** Czcionka: + Tekst podstawowy (Times New Roman)

**Sformatowano:** Czcionka: + Tekst podstawowy (Times New Roman)

**Sformatowano:** Czcionka: + Tekst podstawowy (Times New Roman)

**Sformatowano:** Normalny, Obramowanie: Góra: (Brak obramowania), Dół: (Brak obramowania), Na lewo: (Brak obramowania), Na prawo: (Brak obramowania), Pośrodkowy: (Brak obramowania), Tabulatory: 7,96 cm, Wyśrodkowany + 15,92 cm, Do prawej



<b>Radiation</b>				
- shortwave: downwelling and upwelling - longwave: downwelling and upwelling	CNR4 /Kipp&Zonen	Shortwave: 300 – 2 800 nm Longwave: 4 500 – 42 000 nm	Pyranometer: Uncertainty in daily total < 5% Pyrgeometer: Uncertainty in daily total < 10% ± 6% (-40 – 80°C) ± 25 W m <sup>-2</sup> at 1 000 W m <sup>-2</sup>	09/2010 – 05/2016 (1%)
Downwelling shortwave radiation	SP1110/Skye Campbell Scientific	350 – 1 100 nm	± 5% (typically < 3%)	05/2016 – 05/2020
Datalogger	CR1000/Campbell Scientific	-40 – 50°C		04/2010 – 05/2020 (-)
Ablation and accumulation	SR50/Campbell Scientific	0.5 – 10 m	± 1 cm or 0.4%	9/2010 – 12/2019 (-)

In the 2010/2011 season, data measurement, recording t by the logger was performed every 1 min. Due to high energy demand during the polar night, the sampling time was changed to an instantaneous measurement every 10 minutes. Calibration and testing of sensors were performed regularly during spring expeditions based on the infrastructure of the Polish Polar Station Hornsund.

### 3.2 Glaciological monitoring

In 2009-2010, nine mass-balance stakes were installed on the Werenskioldbreen. The location was locations have been chosen to cover all the glacial zones as well as elevation range from 117 m a.s.l. to 515 m a.s.l. to create longitudinal altitudinal profiles along the northern and southern parts tributaries of the glacier (Figure 1). The stakes not covered the glacier zones from 117 m a.s.l. to 515 m a.s.l.

The stakes, 6 to 8 meters long, were embedded in the glacier by a steam drilling rig or by Kovacs Ice Coring System- (ICS). The mass-balance stakes were measured twice a year (spring-autumn, 2009-2013) during the winter maximum accumulation (April-May) and at the end of the ablation season (September-October) or once a year (at spring, since 2014). The amount measure of winter accumulation was determined during the spring campaigns. The parameters properties of snow cover (bulk snow density, snow depth, SWE—snow water equivalent) were measured in snow pits (a 100 cm<sup>3</sup> snow gauge by Winter Engineering was used to determine the snow density of subsequent layers) or shallow core boreholes (Kovacs ICS). During the measurements, repeated soundings of the snow depth were also performed with avalanche probes. In the absence of the autumn campaign, boreholes have been drilled on near each stake in order to accurately determine the amount of summer ablation and possible summer accumulation. Measurements during the autumn campaign did not always take place after or at the end of the ablation season. This was due to the logistics of the expeditions and the extension of the ablation season. In the case of availability of data from the SR50A sensor, ablation or accumulation corrections were also made if the winter or summer

Sformatowano: Czcionka: + Tekst podstawowy (Times New Roman)

Sformatowana tabela

Sformatowano: Konspekty numerowane + Poziom: 1 + Styl numeracji: Punktator + Wyrównanie: 0,63 cm + Wcięcie: 1,27 cm

Sformatowano: Czcionka: + Tekst podstawowy (Times New Roman)

Sformatowano: Czcionka: + Tekst podstawowy (Times New Roman)

Sformatowano: Czcionka: + Tekst podstawowy (Times New Roman)

Sformatowana tabela

Sformatowano: Czcionka: + Tekst podstawowy (Times New Roman)

Sformatowano: Czcionka: + Tekst podstawowy (Times New Roman)

Sformatowano: Czcionka: + Tekst podstawowy (Times New Roman)

Sformatowano: Czcionka: + Tekst podstawowy (Times New Roman)

Sformatowano: Czcionka: + Tekst podstawowy (Times New Roman)

Sformatowano: Czcionka: + Tekst podstawowy (Times New Roman)

Sformatowano: Czcionka: + Tekst podstawowy (Times New Roman)

Sformatowano: Czcionka: + Tekst podstawowy (Times New Roman)

Sformatowano

Sformatowano

Sformatowano

Sformatowano

Sformatowano

Sformatowano

Sformatowano

Sformatowano

Sformatowano

Sformatowano

Sformatowano

Sformatowano

Sformatowano

season ended later than the date of field observations. ~~In the years 2009-2011, the positions of the stakes were measured with precise GNSS receivers LEICA 1230 to determine glacier velocity. A portion~~Some of the ablation stakes have been damaged every few years. They have been broken by wind, polar bears, melt out from the ice or been buried by snow. The network of ablation stakes was supplemented and renovated ~~as part of ongoing research and projects during maintenance visits.~~ Unfortunately, recent years have resulted in large gaps in measurements due to the pandemic travel restrictions: ~~(years 2020 and 2021).~~ Detailed information on the temporal availability of glaciological data is presented in Table 2.

Sformatowano: Czcionka: + Tekst podstawowy (Times New Roman)

Sformatowano: Czcionka: + Tekst podstawowy (Times New Roman)

Sformatowano: Czcionka: + Tekst podstawowy (Times New Roman)

Table 2. Overview of mass balance and snow cover measurements on ablation stakes and infrastructure maintenance in years 2009-2020 on Werenskioldbreen (Svalbard), where: S – spring campaign (winter balance, April-May), A – autumn campaign (summer balance, August-September, can be performed next year spring), X – lack of stake, SP – snow pit (SWE data), KD – ~~Kovacs~~CS drilling (SWE data), G – GPS measurements, SR50 – automatic measurements at AWS.

Stake no.	1	2 (+AWS)	3	4	5	6	7	8	9
Coordinates (UTM 33N), height (geoid EGM_96)	8556724.662; 512219.566N 8556724; E512219; 515	8554930.167; 510423.846N 8554930; E510423; 384	8558594.6; 510423.846 N8558594; E510423; 471	8557076.138 510048.921 N8557076; E5100481; 392	8554448.524 509786.006 N8554448; E509786; 308	8556047.777 508243.448 N8556047; E508243; 188	8555045.023 507837.608 N8555045; E507837; 199	8553738.705 507697.579 N8553738; E507697; 277	506449.264; 8559956.882 N8559956; E506449; 120
2009	S, A, SP, G	S, A, SP, G	S, A, SP, G	S, A, SP, G	S, A, SP, G	S, A, SP, G	S, A, SP, G	S, A, SP, G	X
2010	S, A, SP, G	S, A, SR50, G	S, A, G	S, A, G	S, A, SP, G	S, A, G	S, A, SP, G	S, A, G	S, A, SP, G
2011	S, A, SP, G	S, A, SR50, G	S, A, SP, G	S, A, SP, G	S, A, G	S, A, G	S, A, SP, G	S, A, SP, G	S, A, G
2012	S, A	S, A, SP, SR50	S-X, A	S-X, A	S-X, A	S, A	S, A, SP	S, A	S, A
2013	S-X, A-X	X, SR50	S, KD, A	S, KD, A	S-X, A-X	S, KD, A	S, SP	S, KD	S-X, A
2014	S, A, SP	X, SR50	S, A	S, A	S, A-X, SP	S, A	S, A, SP	S, A	S, A-X
2015	S, A-X, SP	X, SR50	S, A	S, A	S, A, SP	S, A	S, A	S, A-X	S, A-X, SP
2016	S, A-X, KD	X, KD, SR50	S, A	S, A	S-X, A-X	S, A-X	S, A	S, A	S-X, A-X
2017	S, A	X, KD, SR50	S, A, KD	S, A, KD	S, A, KD	X, A	S, A, KD	S, A	S, A-X, KD
2018	S-X, A, KD	X, KD, SR50	S, A, KD	S, A, KD	S, A	X	S, A, KD	X	S, A, KD
2019	X, KD	X, KD, SR50	S-X	S, A	S, KD, A	X	X, KD	X	S, A, KD
2020	S	X	S	S	S	X	S	X	S

Sformatowano: Czcionka: + Tekst podstawowy (Times New Roman)

Sformatowano: Czcionka: + Tekst podstawowy (Times New Roman)

Sformatowana tabela

Based on the data collected, the following glaciological variables are available: ~~annual and seasonal and annual point ablation and accumulation~~glacier-wide surface mass balance, snow depth, bulk snow density and SWE (snow water equivalent) at the measuring points, ~~surface mass balance and data from automatic measurements (AWS) of ablation and accumulation by the SR50 sonic distance sensor (Campbell Scientific, SR50 L and SR50A L, https://www.campbellsci.com/sr50).~~

Sformatowano: Czcionka: + Tekst podstawowy (Times New Roman)

Sformatowano: Czcionka: + Tekst podstawowy (Times New Roman)

Sformatowano: Czcionka: + Tekst podstawowy (Times New Roman)

Sformatowano: Czcionka: + Tekst podstawowy (Times New Roman)

Sformatowano: Czcionka: + Tekst podstawowy (Times New Roman)

Sformatowano: Czcionka: + Tekst podstawowy (Times New Roman)

Sformatowano: Czcionka: + Tekst podstawowy (Times New Roman)

The analyses of the glacier's surface mass balance excepted field measurements were based on altitude zones determined from digital elevation models (DEM). Two DEMs with geoidal height (EGM2008) were used, one generated from SPOT image

Sformatowano: Normalny, Obramowanie: Góra: (Brak obramowania), Dół: (Brak obramowania), Na lewo: (Brak obramowania), Na prawo: (Brak obramowania), Pośrodku: (Brak obramowania), Tabulatory: 7,96 cm, Wyśrodkowany + 15,92 cm, Do prawej



acquired on 1 September 2008 (Ignatiuk et al., 2014) for years 2008 – 2019 and Pleiades high-resolution images taken on 20 August 2017 (Błaszczuk et al., 2019); for year 2020,

Sformatowano: Czcionka: + Tekst podstawowy (Times New Roman)

Sformatowano: Czcionka: + Tekst podstawowy (Times New Roman)

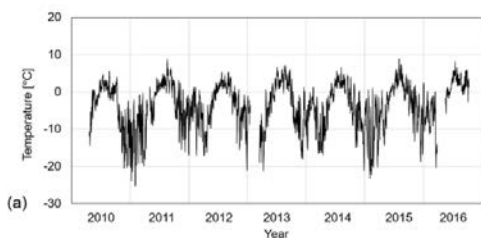
## 4 Meteorological observations

### 4.1 Air temperature and radiation

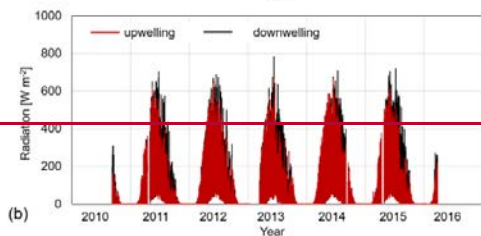
The air temperature data forms the most homogeneous series for 2010-2016 (Figure 2a). In 2017-2020 the data gaps were already significant due to failure a series of failures of the instruments and the lack of servicing due to travel restrictions caused by the COVID-19 pandemic. Also, for 2010-2016, net radiation balance data (short- and long-wave radiation) are available (Figure 2b,c). In 2017-2020, radiation data included only downwelling shortwave radiation.

Sformatowano: Czcionka: + Tekst podstawowy (Times New Roman)

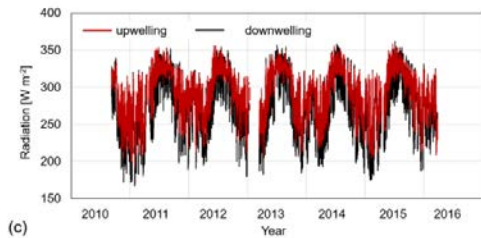
Sformatowano: Czcionka: + Tekst podstawowy (Times New Roman)



(a)



(b)



(c)

Sformatowano: Normalny, Obramowanie: Góra: (Brak obramowania), Dół: (Brak obramowania), Na lewo: (Brak obramowania), Na prawo: (Brak obramowania), Pośrodku : (Brak obramowania), Tabulatory: 7,96 cm, Wyśrodkowany + 15,92 cm, Do prawej



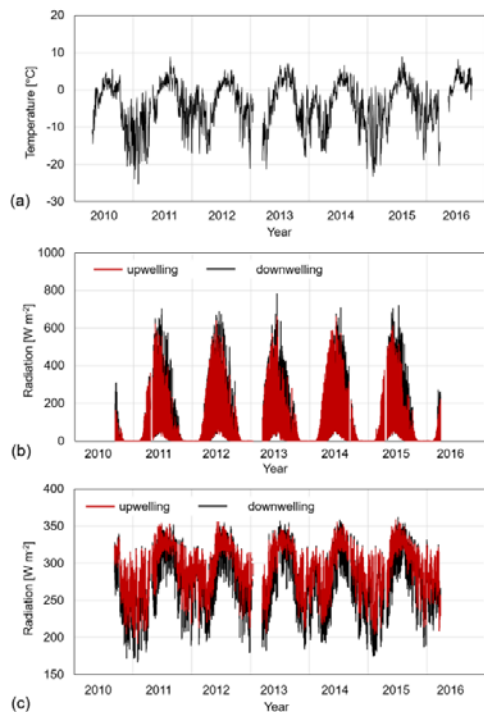


**Figure 2-2: Time series of meteorological variables from 2010 to 2016 on Werenskioldbreen, including daily average air temperature (a), hourly average shortwave radiation (b) and hourly average longwave radiation (c) for downwelling (black line) and upwelling (red line) radiation.**

For years with full data continuity (Figure 2a), air temperature monthly and yearly averages were calculated and then compared with the data from the Polish Polar Station Hornsund (Wawrzyniak and Osuch, 2020). The average difference in the annual temperature (2011, 2012, 2014, 2015) on the glacier (380 m a.s.l.) and the Polish Polar Station Hornsund (8 m a.s.l.) was  $-2.7^{\circ}\text{C}$ , which gives an average temperature lapse rate  $0.72/100\text{ m}$ . The air temperature increased by  $0.09^{\circ}\text{C}$  per year, which is over five times faster than the global average of  $0.17^{\circ}\text{C}$  per decade (NOAA, 2020). More importantly, a twice as high trend of  $0.2^{\circ}\text{C}$  per year is recorded for the summer months (JJA) when glaciers melt most rapidly-between glacier (380 m a.s.l.) and the Polish Polar Station Hornsund (8 m a.s.l.) was  $-2.7^{\circ}\text{C}$ , which gives an average temperature lapse rate  $0.72/100\text{ m}$  (annual values varies from 0.55 to 0.80). We have calculated the significance of the trend presented in this study using the non-

**Sformatowano:** Czcionka: +Tekst podstawowy (Times New Roman), 9 pkt, Pogrubienie, Kolor czcionki: Czarny

**Sformatowano:** Czcionka: +Tekst podstawowy (Times New Roman), 9 pkt, Pogrubienie, Kolor czcionki: Czarny

**Sformatowano:** Normalny, Odstęp Po: 10 pkt, Obramowanie: Góra: (Brak obramowania), Dół: (Brak obramowania), Na lewo: (Brak obramowania), Na prawo: (Brak obramowania), Pośrodkowo: (Brak obramowania)

**Sformatowano:** Czcionka: +Tekst podstawowy (Times New Roman)

**Sformatowano:** Normalny, Obramowanie: Góra: (Brak obramowania), Dół: (Brak obramowania), Na lewo: (Brak obramowania), Na prawo: (Brak obramowania), Pośrodkowo: (Brak obramowania), Tabulatory: 7,96 cm, Wyśrodkowany + 15,92 cm, Do prawej

155 parametric modified Mann – Kendall test (Hamed and Rao, 1998) with considering the effect of autocorrelation of time series. The slope of the trend was calculated using Sen’s method (Sen, 1968). The test indicated the statistically significant increasing temperature trend in the period 2010-2016 (with the significance level  $\alpha = 0.05$  and  $p\text{-value} = 0.036$ ) taking into account the 12-month seasonality the Sen’s slope was 0.02. Gaps in the data were filled based on the relations between air temperature measured on the PPS in Hornsund and air temperature on the WRN glacier ( $R^2 = 0.96$ ). According to the Wawrzyniak & Osuch (2019) estimated slope of trend for air temperature between 1979–2018 at the Hornsund station was estimated as 1.14° C per decade. Increasing distance between the glacier surface and the sensors during the season is affecting on the air temperature measurements. Periodic measurements of the vertical temperature gradient between 0.5 and 4 m carried out at the AWS indicate that the air temperature in the atmospheric boundary layer changes by about 0.2°C per 1 m during the ablation season.

160 Downwelling shortwave radiation reaches its maximum during the middle of the polar day (June). Its annual course is governed by the occurrence of polar day and night, while its daily course is governed by cloudiness and the height of the sun above the horizon. The reflected shortwave radiation (upwelling) is a function of the surface albedo. In the spring and early summer, we observed the highest values of reflected radiation due to the presence of snow cover on the glacier. In the further part of the ablation season (July-August), we noticed a sudden decrease in reflected radiation (Figure 2b) as a result of the disappearance of snow cover at the measurement site (AWS) and the appearance of glacial ice on the surface. The decrease in upwelling shortwave radiation can be slight (e.g. 2012) when the melting of snow cover occurs mainly as a result of surface ablation or abrupt (e.g. 2015) when significant rainfall led to a sudden change in the albedo on the glacier. The maximum values of downwelling/upwelling longwave radiation (Figure 2c) usually occurred in summer and autumn. The values in winter and spring are lower, which in general shows similar patterns with the seasonal variations in air temperature. The values above 316 W m<sup>-2</sup> of outgoing longwave radiation may be caused by the presence of the water under the station or the presence of sediment or cryoconite. Both of these situation were observed at AWS. In the he view of the CNR4 sensor (180o), there is also a mast with a logger, sensors and a solar panel, what cause distorts of the observations. These problems are difficult to eliminate. Assuming the homogeneity of the surface around AWS, increasing the distance of the CNR4 sensor from the glacier surface should not affects its measurements.

#### 4.2 Other variables

180 In 2009-2020, the The AWS measured relative humidity, wind direction and speed, ablation and accumulation of snow. (for the time span see Table 1). These sensors were installed at the station depending on the needs of the ongoing projects and doctoral dissertations. Not all of them could be connected to the datalogger at the same time. Due to their construction, these sensors are also less resistant to operation in polar conditions and to servicing Servicing only once a year, causing a higher failure rate for these sensors. Therefore, the data obtained for these variables are not continuous and not homogenous for the entire observation period. Nevertheless, these data are available and are of great value for solving specific scientific problems-like rain on snow events (Łupikasza et al., 2019) or supplying data to other models (Dacaux et al., 2019).

Sformatowano: Czcionka: +Tekst podstawowy (Times New Roman)

Sformatowano: Czcionka: +Tekst podstawowy (Times New Roman)

Sformatowano: Czcionka: +Tekst podstawowy (Times New Roman)

Sformatowano: Czcionka: +Tekst podstawowy (Times New Roman)

Sformatowano: Czcionka: +Tekst podstawowy (Times New Roman)

Sformatowano: Czcionka: +Tekst podstawowy (Times New Roman)

Sformatowano: Czcionka: +Tekst podstawowy (Times New Roman)

Sformatowano: Czcionka: +Tekst podstawowy (Times New Roman)

Sformatowano: Czcionka: +Tekst podstawowy (Times New Roman)

Sformatowano: Normalny, Obramowanie: Góra: (Brak obramowania), Dół: (Brak obramowania), Na lewo: (Brak obramowania), Na prawo: (Brak obramowania), Pośrodkowy : (Brak obramowania), Tabulatory: 7,96 cm, Wyśrodkowany + 15,92 cm, Do prawej

## 5 Glaciological observations

### 5.1 Point ablation and accumulation

Measurements on mass-balance stakes (Figure 1, Table 2) were performed in accordance with the recommendations and guidelines contained in the Glossary of Glacier Mass Balance and Related Terms (Cogley et al., 2011). After Cogley et al. (2011) it was assumed that accumulation is always positive, while ablation is negative. Therefore, the calculation of the point mass balance is Eq. (1):

$$b_a = c_a + a_a = b_w + b_s = c_w + a_w + c_s + a_s \quad (1)$$

where:  $b_a$  – annual balance at a point,  $c_a$  – annual accumulation,  $a_a$  – annual ablation,  $b_w$  – winter balance,  $b_s$  – summer balance,  $c_w$  – winter accumulation,  $a_w$  – winter ablation,  $c_s$  – summer accumulation,  $a_s$  – summer ablation

As it is a method of determining point mass balance on the glacier surface includes measurements at stakes and in snow pits or boreholes. The high of each stake above snow/ice is difficult to measure measured twice in the annual maximum of winter accumulation and annual at the end of the summer ablation, the winter and summer balance were measured (including the winter. The measurements also include depth probing and summer ablation density sampling of the snow and accumulation). The firm (see section 5.2). They are made at single points, the results from a number of points being extrapolated and integrated to yield the surface mass balance calculation was based on the physical parameters of snow and ice measured in the field (see Snow Water Equivalent) over the entire glacier (Cogley et al., 2011; see section 5.3). The error of point mass balance was estimated using the total differential function: using general equation;

Sformatowano: Czcionka: + Tekst podstawowy (Times New Roman)

Sformatowano: Czcionka: + Tekst podstawowy (Times New Roman)

Sformatowano: Czcionka: + Tekst podstawowy (Times New Roman)

Sformatowano: Czcionka: + Tekst podstawowy (Times New Roman)

Sformatowano: Czcionka: + Tekst podstawowy (Times New Roman)

Sformatowano: Czcionka: + Tekst podstawowy (Times New Roman)

Sformatowano: Czcionka: + Tekst podstawowy (Times New Roman)

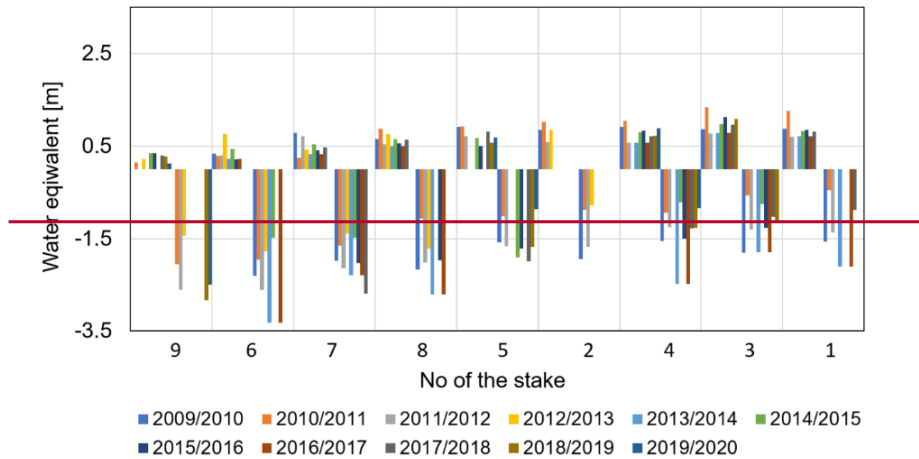
Sformatowano: Czcionka: + Tekst podstawowy (Times New Roman)

Sformatowano: Czcionka: + Tekst podstawowy (Times New Roman)

Sformatowano: Czcionka: + Tekst podstawowy (Times New Roman)

Sformatowano: Czcionka: + Tekst podstawowy (Times New Roman)

Sformatowano: Normalny, Obramowanie: Góra: (Brak obramowania), Dół: (Brak obramowania), Na lewo: (Brak obramowania), Na prawo: (Brak obramowania), Pośrodku: (Brak obramowania), Tabulatory: 7,96 cm, Wyśrodkowany + 15,92 cm, Do prawej



205

$$\Delta f(x_1, x_2, \dots, x_n) = \sqrt{\left(\frac{\partial f}{\partial x_1}\right)^2 (\Delta x_1)^2 + \left(\frac{\partial f}{\partial x_2}\right)^2 (\Delta x_2)^2 + \dots + \left(\frac{\partial f}{\partial x_n}\right)^2 (\Delta x_n)^2} \quad (2)$$

Where:  $\Delta f$ ,  $\Delta x$  – error of the variable,  $\partial f / \partial x_n$  – partial derivative,  $x_1, x_2, \dots, x_n$  – variables.

Base on the eq. (2) we've calculated the error of winter, summer and annual point surface mass balance using equations:

**Sformatowano:** Normalny, Obramowanie: Góra: (Brak obramowania), Dół: (Brak obramowania), Na lewo: (Brak obramowania), Na prawo: (Brak obramowania), Pośrodku : (Brak obramowania), Tabulatory: 7,96 cm, Wyśrodkowany + 15,92 cm, Do prawej

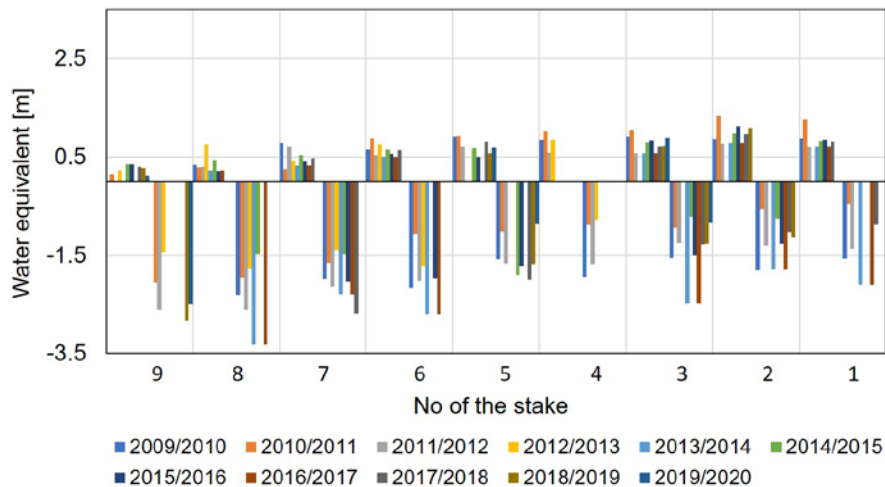


**Figure 3-3: Winter and summer balance at the point on 1-9 mass-balance stakes in years 2009-2020** For the location/elevation of the stake see Figure 1 and Table 2. Stakes have been lined up according to a height above sea level.

The dataset includes point winter and summer mass balance measurements on mass-balance stakes in 2009-2020 and the calculated point annual mass balance. The data allow the analysis of the spatial and seasonal variability of accumulation and ablation at points on the glaciers at different altitudes. The analysis of the winter balance (Figure 3) shows the interannual fluctuations in snow accumulation in the entire altitude profile of the glacier. The analysis of point winter balance shows the smallest interannual fluctuations on the glacier snout (stake 9) and in the sheltered upper glacier cirque (stake 8). In the case of the point summer balance, the greatest interannual changes are observed in the middle zone of the glacier (200 – 400 m a.s.l.). This is due to a longer ablation period and higher temperatures not previously recorded at these altitudes. The variability of the annual surface mass balance is dominated by the summer surface mass balance (Østby et al., 2011; Grabiec et al., 2012; Van Pelt et al., 2019).

**Sformatowano:** Czcionka: +Tekst podstawowy (Times New Roman), 9 pkt, Pogrubienie, Kolor czcionki: Czarny

**Sformatowano:** Czcionka: +Tekst podstawowy (Times New Roman), 9 pkt, Pogrubienie, Kolor czcionki: Czarny

**Sformatowano:** Normalny, Odstęp Po: 10 pkt, Obramowanie: Góra: (Brak obramowania), Dół: (Brak obramowania), Na lewo: (Brak obramowania), Na prawo: (Brak obramowania), Pośrodku: (Brak obramowania)

**Sformatowano:** Czcionka: +Tekst podstawowy (Times New Roman), 9 pkt, Pogrubienie, Kolor czcionki: Czarny

**Sformatowano:** Czcionka: +Tekst podstawowy (Times New Roman)

**Sformatowano:** Czcionka: +Tekst podstawowy (Times New Roman)

**Sformatowano:** Normalny, Obramowanie: Góra: (Brak obramowania), Dół: (Brak obramowania), Na lewo: (Brak obramowania), Na prawo: (Brak obramowania), Pośrodku: (Brak obramowania), Tabulatory: 7,96 cm, Wyśrodkowany + 15,92 cm, Do prawej

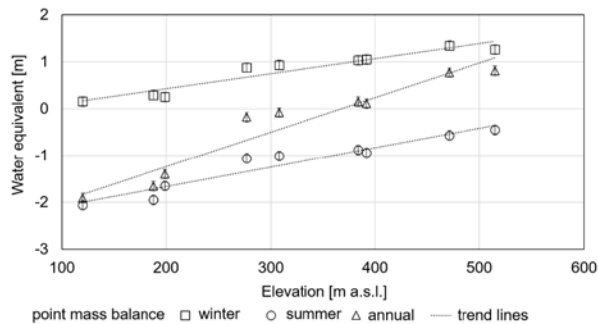
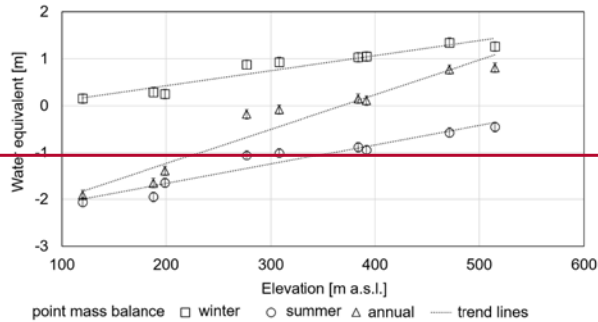


**Figure 4-4: Examples of winter, summer and annual point mass balance on Werenskioldbreen (season 2010/2011). Whiskers show an error: (total differential function).**

Each of the balance years can be considered separately (Figure 4). Winter accumulation in the analysed period was generally sparse/low. The last significant accumulation on Werenskioldbreen took place in 2011. A slight accumulation in the highest parts of the glacier was also observed in 2013, 2015 and 2020. Observations from 2020, however, may be biased by unqualified substitutive observers due to the pandemic situation. In all other years, the ELA was above the highest monitored stake, no 1 (Table 2). The data on point mass balance components are crucial for calculations of the general-superficial-glacier-wide surface mass balance-of-glaciers. These data have very high importance for different modelling purposes, e.g. hydrology and glacier drainage modelling, total water discharge from the glacier, sea level rise models and validation of remote sensing products.

Sformatowano: Czcionka: +Tekst podstawowy (Times New Roman), 9 pkt, Pogrubienie, Kolor czcionki: Czarny

Sformatowano: Normalny, Odstęp Po: 10 pkt, Obramowanie: Góra: (Brak obramowania), Dół: (Brak obramowania), Na lewo: (Brak obramowania), Na prawo: (Brak obramowania), Pośrodkowo: (Brak obramowania)

Sformatowano: Czcionka: +Tekst podstawowy (Times New Roman), 9 pkt, Pogrubienie, Kolor czcionki: Czarny

Sformatowano: Czcionka: +Tekst podstawowy (Times New Roman), 9 pkt, Pogrubienie, Kolor czcionki: Czarny

Sformatowano: Czcionka: +Tekst podstawowy (Times New Roman)

Sformatowano: Czcionka: +Tekst podstawowy (Times New Roman)

Sformatowano: Czcionka: +Tekst podstawowy (Times New Roman)

Sformatowano: Czcionka: +Tekst podstawowy (Times New Roman)

Sformatowano: Normalny, Obramowanie: Góra: (Brak obramowania), Dół: (Brak obramowania), Na lewo: (Brak obramowania), Na prawo: (Brak obramowania), Pośrodkowo: (Brak obramowania), Tabulatory: 7,96 cm, Wyśrodkowany + 15,92 cm, Do prawej

## 5.2 Snow Water Equivalent (SWE)

In the years 2009-2019, 49 samplings (shallow drilling or snowpits) were made on the glacier during the spring measurement campaigns in order to determine the bulk snow density, and thus SWE. In the case of snowpit measurements, the density was measured for each homogeneous layer. The bulk snow density for the snow profile was then calculated based on averaged weighted average by layer thickness.

Whereas the bulk snow density during the drilling of snow cores was calculated based on the length and weight of each core in the profile. The SWE was calculated after based on the following equation (Sturm et al. (2010)-):

$$SWE = h_s \frac{\rho_s}{\rho_w} \quad (3)$$

$$\Delta SWE = SWE \sqrt{\left(\frac{\Delta h_s}{h_s}\right)^2 + \left(\frac{\Delta \rho_s}{\rho_s}\right)^2} \quad (4)$$

Where:  $h_s$  – snow depth [m],  $\rho_s$  – bulk snow density [ $\text{kg m}^{-3}$ ],  $\rho_w$  – density of water [ $\text{kg m}^{-3}$ ],  $\Delta h_s$  – error of the snow depth [0.01 m],  $\Delta \rho_s$  – error of the bulk snow density [ $\text{kg m}^{-3}$ ].

The average density of snow cover ranges from 386 to 447  $\text{kg m}^{-3}$  (Table 3). The highest snow density values were noted in 2012. They are related to the extremely warm conditions in the winter season 2011/2012 with the heavy rainfall (Łupikasza et al., 2019) during the winter and caused probably by the inflow of warm Atlantic water (the fjords of south-west Spitsbergen did not freeze).

Table 3. Average snow depth and bulk snow density based upon data from sampling points (snow pits and drilling cores) on Werenskioldbreen in years 2009-2019.

Year	2009	2010	2011	2012	2013	2014	2015	2016	2017	2018	2019
Number of sampling	8	3	5	2	6	3	3	2	6	4	7
Average snow depth [m]	1.79	1.90	1.65	1.35	1.06	1.73	1.57	1.90	1.64	1.53	1.60
Average bulk snow density [ $\text{kg/m}^3$ ]	434	415	412	447	386	391	387	407	427	419	410

Sformatowano: Czcionka: + Tekst podstawowy (Times New Roman)

Sformatowano: Czcionka: + Tekst podstawowy (Times New Roman)

Sformatowano: Czcionka: + Tekst podstawowy (Times New Roman)

Sformatowano: Czcionka: + Tekst podstawowy (Times New Roman)

Sformatowano: Czcionka: + Tekst podstawowy (Times New Roman)

Sformatowano: Czcionka: + Tekst podstawowy (Times New Roman)

Sformatowano: Czcionka: + Tekst podstawowy (Times New Roman)

Sformatowana tabela

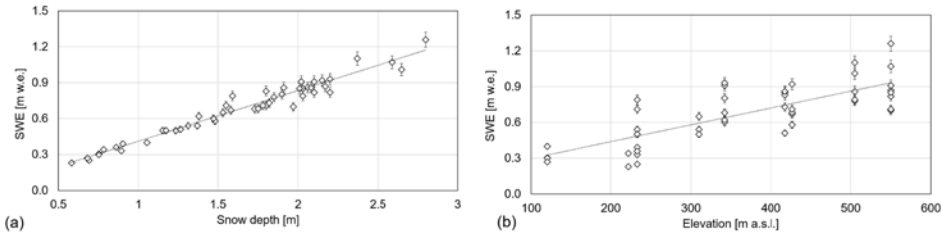
Sformatowano: Czcionka: + Tekst podstawowy (Times New Roman)

Sformatowano: Czcionka: + Tekst podstawowy (Times New Roman)

Sformatowano: Czcionka: + Tekst podstawowy (Times New Roman)

Sformatowano: Normalny, Obramowanie: Góra: (Brak obramowania), Dół: (Brak obramowania), Na lewo: (Brak obramowania), Na prawo: (Brak obramowania), Pośrodku: (Brak obramowania), Tabulatory: 7,96 cm, Wyśrodkowany + 15,92 cm, Do prawej





Avarange

SWE [m w.e.] 0.77 0.81 0.68 0.61 0.52 0.68 0.61 0.79 0.71 0.64 0.65

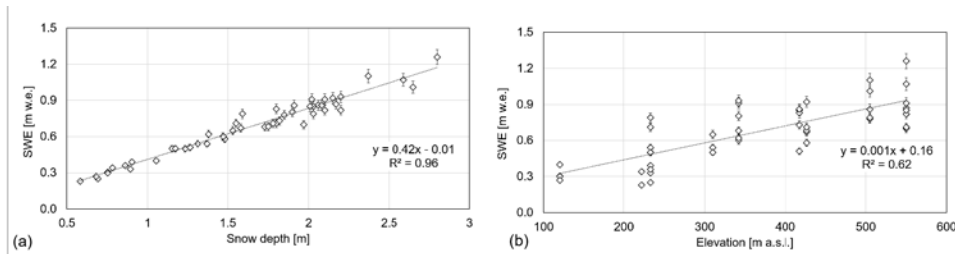


Figure 5:5: Relationship between SWE and snow depth (a) and SWE and elevation m a.s.l. (b). Whiskers show an error. (total differential function, eq.4)

SWE values show a very high correlation with the snow depth ( $R^2 = 0.96$ , Figure 5a) and lower correlation with the altitude above sea level ( $R^2 = 0.62$ , Figure 5b). Uszczyk et al. (2019) found the relationship between the bulk snow density and the snow depth on Hansbreen located next to Werenskioldbreen. It was observed that the bulk snow density increases with snow depth. The long-term data collected on Werenskioldbreen has not confirmed this correlation. In fact, in some seasons it is the opposite, i.e. the low thickness thinner snow cover in the lower zones of the glacier has the highest bulk snow density. Seasonal variability can be explained by various meteorological conditions during the accumulation season. The differences between Werenskioldbreen and Hansbreen can most likely be explained by different orographic conditions and exposure, which affects snow blowing and snow deposition.

Sformatowano: Czcionka: +Tekst podstawowy (Times New Roman), 9 pkt, Pogrubienie, Kolor czcionki: Czarny

Sformatowano: Czcionka: +Tekst podstawowy (Times New Roman), 9 pkt, Pogrubienie, Kolor czcionki: Czarny

Sformatowano: Normalny, Odstęp Po: 10 pkt, Obramowanie: Góra: (Brak obramowania), Dół: (Brak obramowania), Na lewo: (Brak obramowania), Na prawo: (Brak obramowania), Pośrodkowo: (Brak obramowania)

Sformatowano: Czcionka: +Tekst podstawowy (Times New Roman), 9 pkt, Pogrubienie, Kolor czcionki: Czarny

Sformatowano: Czcionka: +Tekst podstawowy (Times New Roman)

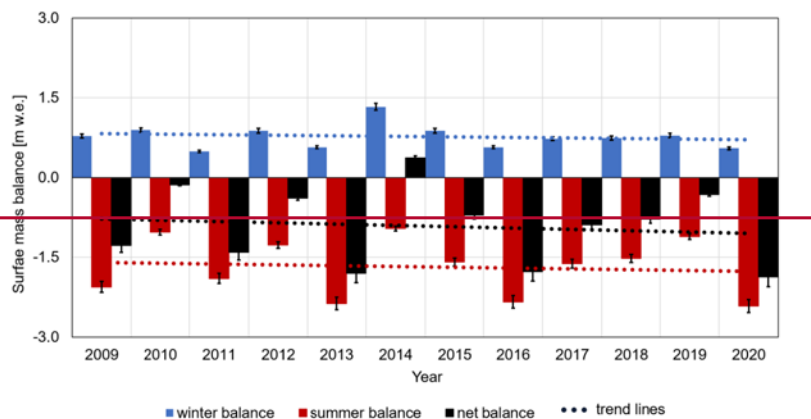
Sformatowano: Czcionka: +Tekst podstawowy (Times New Roman)

Sformatowano: Czcionka: +Tekst podstawowy (Times New Roman)

Sformatowano: Normalny, Obramowanie: Góra: (Brak obramowania), Dół: (Brak obramowania), Na lewo: (Brak obramowania), Na prawo: (Brak obramowania), Pośrodkowo: (Brak obramowania), Tabulatory: 7,96 cm, Wyśrodkowany + 15,92 cm, Do prawej

### 5.3 Surface Glacier-wide surface mass balance (SMB)

While the mass balance is measured on many glaciers, the data series rarely exceeds 10 years (Schuler et al., 2020). Multi-year data series, such as those from Werenskioldbreen, represent a unique value for tracking long-term changes in the Arctic environment. Calculation of the SMB mass balance was based on point winter and summer balance analyses and digital elevation models. The point measurements are extrapolated over the glacier surface determining the balance as a function of altitude and averaging them, using the weights determined from the distribution of the glacier surface as a function of altitude (Cogley et al., 2011). The error was estimated using the total differential function.



Sformatowano: Czcionka: + Tekst podstawowy (Times New Roman)

Sformatowano: Czcionka: + Tekst podstawowy (Times New Roman)

Sformatowano: Czcionka: + Tekst podstawowy (Times New Roman)

Sformatowano: Normalny, Obramowanie: Góra: (Brak obramowania), Dół: (Brak obramowania), Na lewo: (Brak obramowania), Na prawo: (Brak obramowania), Pośrodku: (Brak obramowania), Tabulatory: 7,96 cm, Wyśrodkowany + 15,92 cm, Do prawej

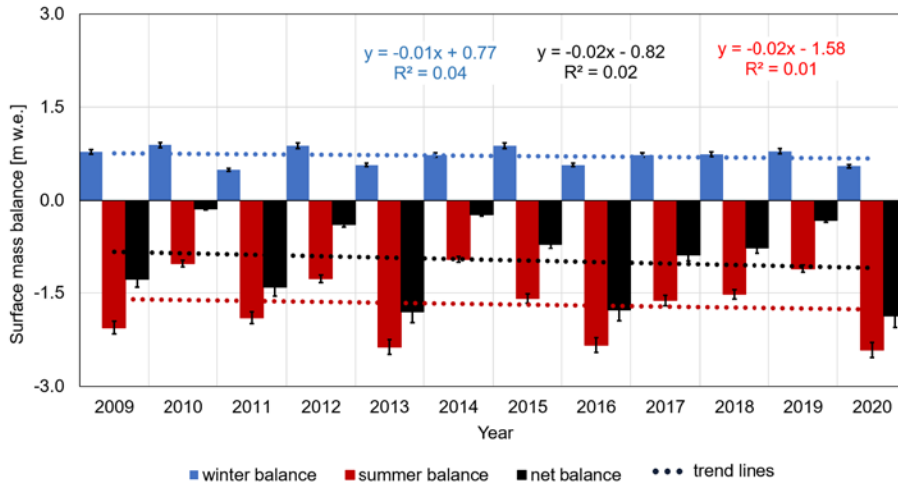


Figure 6-6: Annual surface mass balance and its components of Werenskioldbreen in 2009-2020. Blue bars - winter mass balance, red bars - summer mass balance, green bars - net mass balance. The results for 2019 may be understated (field measurements performed by the non-expert crew).

The long-term trends in the summer and winter SMB indicate increasing summer ablation and decreasing winter accumulation. The largest fluctuations are observed in the summer balance, which depends on the interannual changes in the duration of the positive air temperatures and thus the length of the ablation season. The winter balance shows greater stability, however, over the decade, the trend in the amount of snow accumulation is downward. This entails a negative trend in the SMB surface mass balance of Werenskioldbreen (Figure 6). Based on the trend lines, it can be concluded that winter balance acceleration of mass loss decreases by 0.09 m w.e. per decade, while the summer balance increases/decreases by -0.14 m w.e. for a decade. This gives us an acceleration of the ablation (SMB) by 0.23 m w.e. for a decade on Werenskioldbreen.

The significance of the trends using the non-parametric modified Mann – Kendall test (Hamed and Rao, 1998) showed there is no statistically significant trend in 2009-2020 ( $\alpha = 0.05$ ). The Sen's slope was -0.01, -0.12 and -0.02 for winter, summer and annual glacier-wide mass balance respectively. Hagen et al. (2012) shown that it is impossible to give any trend for the glacier mass balance data for so short time period.

Grabiec et al. (2012) has used monthly values of air temperature and precipitation from the meteorological station at Hornsund and the reanalysis ERA-40 data to hindcast the mass balance of Werenskioldbreen for the years 1959-2002. The average winter SMB for 1959-2002, depending on The average correlation coefficient of the modelled and observed mass balance in the 5

Sformatowano: Czcionka: +Tekst podstawowy (Times New Roman), 9 pkt, Pogrubienie, Kolor czcionki: Czarny

Sformatowano: Czcionka: +Tekst podstawowy (Times New Roman), 9 pkt, Pogrubienie, Kolor czcionki: Czarny

Sformatowano: Czcionka: +Tekst podstawowy (Times New Roman), 9 pkt, Pogrubienie, Kolor czcionki: Czarny

Sformatowano: Normalny, Odstęp Po: 10 pkt, Obramowanie: Góra: (Brak obramowania), Dół: (Brak obramowania), Na lewo: (Brak obramowania), Na prawo: (Brak obramowania), Pośrodkowy: (Brak obramowania)

Sformatowano: Czcionka: +Tekst podstawowy (Times New Roman), 9 pkt, Pogrubienie, Kolor czcionki: Czarny

Sformatowano: Czcionka: +Tekst podstawowy (Times New Roman), 9 pkt, Pogrubienie, Kolor czcionki: Czarny

Sformatowano: Czcionka: +Tekst podstawowy (Times New Roman)

Sformatowano: Czcionka: +Tekst podstawowy (Times New Roman)

Sformatowano: Czcionka: +Tekst podstawowy (Times New Roman)

Sformatowano: Czcionka: +Tekst podstawowy (Times New Roman)

Sformatowano: Czcionka: +Tekst podstawowy (Times New Roman)

Sformatowano: Czcionka: +Tekst podstawowy (Times New Roman)

Sformatowano: Czcionka: +Tekst podstawowy (Times New Roman)

Sformatowano: Normalny, Obramowanie: Góra: (Brak obramowania), Dół: (Brak obramowania), Na lewo: (Brak obramowania), Na prawo: (Brak obramowania), Pośrodkowy: (Brak obramowania), Tabulatory: 7,96 cm, Wyśrodkowany + 15,92 cm, Do prawej



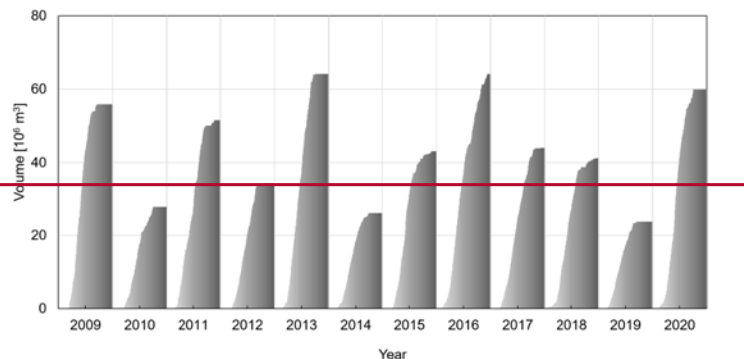


Figure 7: Calculated daily surface

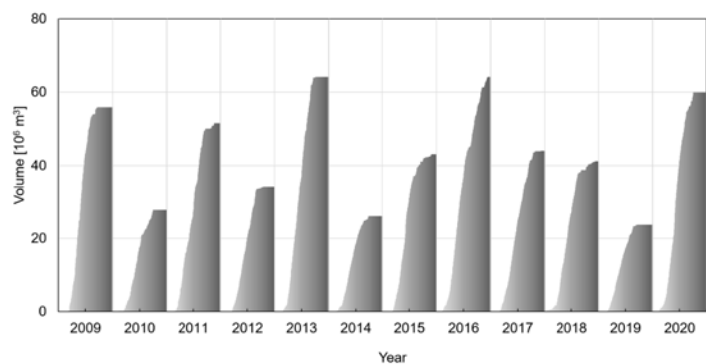


Figure 7: Cumulative ablation [ $10^6 \text{ m}^3$ ] in May – November (2009 – 2020) for Werenskioldbreen.

Seasonal sums of surface ablation oscillate between about  $23.7 \pm 1.7$  (2019) and  $64.2 \pm 4.5 \cdot 10^6 \text{ m}^3$  (2013), with an average of  $44.7 \pm 3.1 \cdot 10^6 \text{ m}^3$  for 2009-2020. The value in 2019 may be underestimated due to problems with field measurements caused by the pandemic travel restrictions. The length of the ablation season determines the size of ablative outflow-meltwater runoff volumes. It varied in the analysed period from 134 days in 2014 to 203 days in 2016 (the average for 2009-2020 was 163 days). The surface ablation is affected by the decrease in the number of sunny days and the increase of days with precipitation and cloud cover (Wawrzyniak and Osuch, 2020). The amount of water produced by surface ablation is the largest

20  
20

Sformatowano: Czcionka: +Tekst podstawowy (Times New Roman), 9 pkt, Pogrubienie, Kolor czcionki: Czarny

Sformatowano: Normalny, Odstęp Po: 10 pkt, Obramowanie: Góra: (Brak obramowania), Dół: (Brak obramowania), Na lewo: (Brak obramowania), Na prawo: (Brak obramowania), Pomiedzy: (Brak obramowania)

Sformatowano: Czcionka: +Tekst podstawowy (Times New Roman)

Sformatowano: Czcionka: +Tekst podstawowy (Times New Roman)

Sformatowano: Czcionka: +Tekst podstawowy (Times New Roman)

Sformatowano: Czcionka: +Tekst podstawowy (Times New Roman)

Sformatowano: Czcionka: +Tekst podstawowy (Times New Roman)

Sformatowano: Normalny, Obramowanie: Góra: (Brak obramowania), Dół: (Brak obramowania), Na lewo: (Brak obramowania), Na prawo: (Brak obramowania), Pomiedzy: (Brak obramowania), Tabulatory: 7,96 cm, Wyrodkowany + 15,92 cm, Do prawej

component of the total runoff from the catchment but precipitation can also be an important element of the water balance (Majchrowska et al., 2015).

## 6 Quality control and data processing

330 Data quality assurance includes additional measurements and calibration of equipment performed during the observation period and post-processing of the collected data. The analysis differed for the meteorological data constituting the time series and for the glaciological data.

335 The first stage of quality control for meteorological data consisted in visualizing each of the measurement series and ~~review~~ ~~re~~reviewing the disrupted data caused by interruptions in the operation of sensors. Due to its location, the automatic measurement station (AWS) operating on Werenskioldbreen could not be ~~monitored~~ ~~maintained~~ with high frequency. As a result there were periodic problems with the power supply as well as with freezing of some sensors. Power shortages manifested themselves in the disappearance of measurements and the occurrence of isolated measurements, the correctness of which could not be confirmed, and therefore they were removed. Similarly, ~~freezing~~ ~~malfunctioning~~ of sensors manifested in 'blocking' the measurement at one value for a longer time. It mainly concerned wind speed ~~and direction~~ measurements. As

340 such values are unnatural, they were identified as erroneous and removed from the set during visual inspection. The next stage of the control was the identification of individual measurements where the values were too different compared with the previous and following measurements and that did not fit in the short-term trend. These ~~measuring pins~~ ~~data spikes~~ were averaged with respect to adjacent measurements. It mainly concerned air temperature and humidity records, where such ~~spikes~~ ~~are believed to be artefacts in the measurement series are unnatural~~. Similarly, the analysis of the measurement series was performed in terms of unnatural values, i.e. values exceeding the permissible variability of the relative humidity or air temperature. These were a few cases. In these situations, such values were eliminated or averaged over adjacent measurements.

345 In the last step, the same variables were compared, ~~but with records~~ from ~~different~~ ~~other~~ weather stations in Svalbard. Air temperature time series have been tested with observations at the Polish Polar Station Hornsund (Wawrzyniak and Osuch, 2020). Mainly, the correlations of the variability of parameters were checked in comparison to the stations accepted as reference. Nevertheless, it should be remembered that even in the case of close points, this correlation does not have to be high or consistent due to the specificity of these stations, i.e. different shading conditions, ground, topography or exposure.

350 Analysis of collected data revealed some imperfections in 10-minutes measurements of the air humidity. There have been some measurements that slightly exceeded the value of 100%. In this case, one of two procedures was undertaken. If the neighbouring measurements to the questionable record show high air humidity – the exceeding value was reduced to 100%. If the neighbouring measurements to the questionable measurement show low air humidity the value was averaged from these neighbouring measurements.

355 A separate analysed issue is the variability/fluctuation of measurements in this 10-minute series. A series of unjustified peaks in the measured values were identified, with a relatively small variability of the parameters recorded by the sensors earlier and

Sformatowano: Czcionka: +Tekst podstawowy (Times New Roman)

Sformatowano: Czcionka: +Tekst podstawowy (Times New Roman)

Sformatowano: Czcionka: +Tekst podstawowy (Times New Roman)

Sformatowano: Czcionka: +Tekst podstawowy (Times New Roman)

Sformatowano: Czcionka: +Tekst podstawowy (Times New Roman)

Sformatowano: Czcionka: +Tekst podstawowy (Times New Roman)

Sformatowano: Czcionka: +Tekst podstawowy (Times New Roman)

Sformatowano: Czcionka: +Tekst podstawowy (Times New Roman)

Sformatowano: Czcionka: +Tekst podstawowy (Times New Roman)

Sformatowano: Czcionka: +Tekst podstawowy (Times New Roman)

Sformatowano: Normalny, Obramowanie: Góra: (Brak obramowania), Dół: (Brak obramowania), Na lewo: (Brak obramowania), Na prawo: (Brak obramowania), Pośrodku : (Brak obramowania), Tabulatory: 7,96 cm, Wyśrodkowany + 15,92 cm, Do prawej

360 later. The sites for this potential correction were searched for when reviewing the series on the chart. At the time of identifying such a value, the variability of consecutive measurements was analysed. 12 measurements were analysed before the questioned measurement ( $\pm 2$  hours). In this situation, when these fluctuations exceeded 2 standard deviations of the variability, they were averaged with the direct measurements before and after the questioned measurement. When more than 3 standard deviations of the measurements assessed according to this criterion were registered, directly after each other, they were completely removed and marked in the published files by missing values (described in the attributes of NetCDF files). This procedure was used for both air humidity and temperature. The tested measurements were compared, if possible, with their counterparts measured at the station in Hornsund, for similar dynamics of variation, which could justify a similar dynamics of variability in the published measurement series. When a large dynamics of the variability of the measured parameters were identified in both locations, the criterion of 3 standard deviations was used instead of the previously described 2SD. Unfortunately, the conditions of the measuring station in Hornsund are very different from the location on the glacier. For this reason, the direct possibility of comparing measurements between these locations may be limited only to the analysis of short-term trends and dynamics of the variability of both air temperature and humidity. The stations differ in height above sea level, distance from the sea, and the ground on which they are located.

375 In the case of wind measurements, the most common problem was the one resulting from the sensor icing, which manifested itself in recording the same value over a longer period. The only possible correction here was to remove erroneous values throughout the occurrence.

In the case of radiation measurements, the fewest corrections were made as these sensors proved to be the most reliable. The introduced corrections concerned only sporadic jumps in the measured parameters. However, in this case, due to the large impact of cloudiness on the measured parameters, which may be marked in the measurements, only the evident cases were removed or averaged with such fluctuations. Jumps of single measurements against a background of relatively low long-term variability were identified as such cases.

380 Measurement series prepared and tested in such a way were used to calculate series with an hourly and daily resolution (24h). The series was created as a result of averaging or summing up depending on the parameter under development. In the case of wind direction, it was limited only to calculating the direction of the mean wind vector in hourly intervals.

385 Such prepared Glaciological data are not collected automatically in large amounts but are based on single, unique observations that must be made with great care as they are not possible to repeat or relate to observations from other areas.

390 Each measurement of the ablation stake was performed twice. If the funnel melts in ice or snow around the stake, the measurement was made to the theoretical flat surface joining the edges of the funnel. In the event of a stake skewing, its total length was measured and then, if possible, the stake was replaced with a new one. Measurements of the snow depth, apart from making snow pits or shallow drilling, were always verified by taking 2-3 measurements with an avalanche probe. In order to obtain comparable measurements of bulk snow density (and SWE) these measurements were performed with two different methods (snow pit and shallow drilling), and a series of parallel measurements were performed showing that the difference in

Sformatowano: Czcionka: +Tekst podstawowy (Times New Roman)

Sformatowano: Czcionka: +Tekst podstawowy (Times New Roman)

Sformatowano: Czcionka: +Tekst podstawowy (Times New Roman)

Sformatowano: Normalny, Obramowanie: Góra: (Brak obramowania), Dół: (Brak obramowania), Na lewo: (Brak obramowania), Na prawo: (Brak obramowania), Pośrodku : (Brak obramowania), Tabulatory: 7,96 cm, Wyśrodkowany + 15,92 cm, Do prawej



the calculated SWE does not exceed 5%. In order to obtain the most accurate data from the ICS drill, the quality of the obtained ice and snow cores was checked in order to determine the precise diameter of the obtained cores.

The obtained point and glacier-wide surface mass balance calculations were compared with the data published by the World Glacier Monitoring Service (<https://wgms.ch>) for other glaciers on Svalbard in order to verify the consistency of trends (Schuler et al., 2020). Data on surface ablation in seasons where it was possible were controlled by comparison with the data collected by the SR50 (sonic ranger) sensor, which was also used to verify the duration of the ablation season. The glaciological data were saved in the CSV files.

The quality of DEM generated from the SPOT images in 2008 was validated with the height of stakes on Werenskioldbreen (Ignatiuk et al., 2014). The median value and standard deviation of the accuracy of the DEM were -0,85 m and 2,2 m, respectively. Validation of the DEM generated from Pleiades images taken in 2017 was based on stake positions over neighbouring Hansbreen (Błaszczuk et al. 2019). The median value and standard deviation of DEM accuracy were -0,36 m and 0,24 m, respectively.

## **7. Dataset structure**

Prepared measurement series were saved in the NetCDF (Network Common Data Form) format and placed on the server supporting OPeNDAP ([www.ppdb.us.edu.pl](http://www.ppdb.us.edu.pl)). The choice of this type of file is due to its universal nature. NetCDF files are in line with the modern trend of storing and publishing measurement series meeting the FAIR data principles. The collections are compliant with Unidata's Attribute Convention for Dataset Discovery (ACDD-1.3) and Climate and Forecast (CF) Conventions (CF-1.8). The Attribute Convention for Dataset Discovery identify and define a list of NetCDF global attributes recommended for describing a NetCDF dataset to discovery systems such as Digital Libraries. Software tools can use these attributes for extracting metadata from datasets, and exporting to Dublin Core, DIF, ADN, FGDC, ISO 19115 etc. metadata formats. The CF metadata conventions are designed to promote the processing and sharing files created with the NetCDF API. The conventions define metadata that provide a definitive description of what the data in each variable represents and the spatial and temporal properties of the data. This enables users of data from different sources to decide which quantities are comparable and facilitates building applications with powerful extraction, regridding, and display capabilities. The CF convention includes a standard name table, which defines strings that identify physical quantities. Global Attributes of prepared NetCDF files comply with the recommendations of The Arctic Data Center (ADC) which is a service provided by the Norwegian Meteorological Institute (MET) (<https://adc.met.no/node/4>).

All ACDD 1.3 Variable Attributes recommended were used. They were supplemented with the so-called \_FillValue = -999.9 indicating data gaps and valid\_max and valid\_min describing the natural and allowed variability of these parameters in the measurement area. All measurement parameter names follow Climate and Forecast (CF) Standard Name Table version 77 which was available on the day when the dataset was published.

**Sformatowano:** Czcionka: +Tekst podstawowy (Times New Roman)

**Sformatowano:** Czcionka: +Tekst podstawowy (Times New Roman)

**Sformatowano:** Czcionka: +Tekst podstawowy (Times New Roman)

**Sformatowano:** Normalny, Obramowanie: Góra: (Brak obramowania), Dół: (Brak obramowania), Na lewo: (Brak obramowania), Na prawo: (Brak obramowania), Pośrodku: (Brak obramowania), Tabulatory: 7,96 cm, Wyśrodkowany + 15,92 cm, Do prawej

The keywords vocabulary used is consistent with the Global Change Master Directory (GCMD) Keywords (https://earthdata.nasa.gov/earth-observation-data/find-data/idn) developed for 20 years by The National Aeronautics and Space Administration (NASA)/gcmd-keywords) which are a hierarchical set of controlled Earth Science vocabularies that help ensure Earth science data, services, and variables are described in a consistent and comprehensive manner and allow for the precise searching of metadata and subsequent retrieval of data, services, and variables.

~~Glaciological data have different specifics than meteorological data. 8. Glaciological data are not collected automatically in large amounts but are based on single, unique observations that must be made with great care as they are not possible to repeat or relate to observations from other areas.~~

~~Each measurement of the ablation stake was performed twice. If the funnel melts in ice or snow around the stake, the measurement was made to the theoretical flat surface joining the edges of the funnel. In the event of a stake skewing, its total length was measured and then, if possible, the stake was replaced with a new one. Measurements of the snow depth, apart from making snow pits or shallow drilling, were always verified by taking 2-3 measurements with an avalanche probe. In order to obtain comparable measurements of bulk snow density (and SWE) these measurements were performed with two different methods (snow pit and shallow drilling), and a series of parallel measurements were performed showing that the difference in the calculated SWE does not exceed 5%. In order to obtain the most accurate data from the Kovaes drill, the quality of the obtained ice and snow cores was checked in order to determine the precise diameter of the obtained cores.~~

~~The obtained SMB and point mass balance calculations were compared with the data published by the World Glacier Monitoring Service (https://wgms.ch) for other glaciers on Svalbard in order to verify the consistency of trends and qualitative and quantitative control. Data on surface ablation in seasons where it was possible were controlled by comparison with the data collected by the SR50 (sonic ranger) sensor, which was also used to verify the duration of the ablation season. Measurements during the autumn campaign did not always take place after or at the end of the ablation season. This was due to the logistics of the expeditions and the extension of the ablation season. An SR50 sensor was used to control the quality of the collected ablation data, or additional drillings were made during the next spring expedition to verify the ablation data collected in the previous year. The glaciological data were saved in the CSV and NetCDF formats using GCMD keywords vocabulary.~~

~~The quality of DEM generated from the SPOT images in 2008 was validated with the height of stakes on Werenskioldbreen (Ignatiuk et al., 2014). The median value and standard deviation of the accuracy of the DEM were -0,85 m and 2.2 m, respectively. Validation of the DEM generated from Pleiades images taken in 2017 was based on stake positions over neighbouring Hansbreen (Błaszczyk et al. 2019). The median value and standard deviation of DEM accuracy were -0,36 m and 0.24 m, respectively.~~

**Sformatowano:** Czcionka: + Tekst podstawowy (Times New Roman), 11 pkt

**Sformatowano:** Czcionka: + Tekst podstawowy (Times New Roman), 11 pkt

**Sformatowano:** Czcionka: + Tekst podstawowy (Times New Roman)

**Sformatowano:** Czcionka: + Tekst podstawowy (Times New Roman), 11 pkt

**Sformatowano:** Czcionka: + Tekst podstawowy (Times New Roman)

**Sformatowano:** Normalny, Obramowanie: Góra: (Brak obramowania), Dół: (Brak obramowania), Na lewo: (Brak obramowania), Na prawo: (Brak obramowania), Pośrodkowy : (Brak obramowania), Tabulatory: 7,96 cm, Wyśrodkowany + 15,92 cm, Do prawej

## 7. Data availability

The data is stored in two repositories that provide long-term availability, open access, DOI and license according to the FAIR principles: Zenodo ([www.zenodo.org](http://www.zenodo.org)):

~~and Polish Polar Database (<https://ppdb.us.edu.pl>)~~, meteorological data: <https://doi.org/10.5281/zenodo.5791748> (Ignatiuk, 2021a), glaciological data: <https://doi.org/10.5281/zenodo.5792168> (Ignatiuk, 2021b).

~~and Polish Polar Database (<https://ppdb.us.edu.pl>):~~

Air temperature:

<https://ppdb.us.edu.pl/geonetwork/srv/pol/catalog.search;jsessionid=7A0C3C8EAEA1B8F61D8F0B57177B7098#/metadata/abc6becf-97f0-4dca-b597-2fa3438f43ab>

Relative humidity:

<https://ppdb.us.edu.pl/geonetwork/srv/pol/catalog.search;jsessionid=7A0C3C8EAEA1B8F61D8F0B57177B7098#/metadata/bdd6b724-d75c-49a1-83c6-eb2007107cde>

Wind speed:

<https://ppdb.us.edu.pl/geonetwork/srv/pol/catalog.search;jsessionid=7A0C3C8EAEA1B8F61D8F0B57177B7098#/metadata/d0ad64ab-ad70-43d7-9383-8a9213e6c40f>

Shortwave flux:

<https://ppdb.us.edu.pl/geonetwork/srv/pol/catalog.search;jsessionid=7A0C3C8EAEA1B8F61D8F0B57177B7098#/metadata/12ed9717-8cd7-4583-b2c6-089d50e6ad61>

<https://ppdb.us.edu.pl/geonetwork/srv/pol/catalog.search;jsessionid=7A0C3C8EAEA1B8F61D8F0B57177B7098#/metadata/fa3bd41b-dfbb-49e8-bdf6-7c56e9bb902f>

Longwave flux:

<https://ppdb.us.edu.pl/geonetwork/srv/pol/catalog.search;jsessionid=7A0C3C8EAEA1B8F61D8F0B57177B7098#/metadata/9309a6b1-663c-4227-9eb6-39761c1d868d>

<https://ppdb.us.edu.pl/geonetwork/srv/pol/catalog.search;jsessionid=7A0C3C8EAEA1B8F61D8F0B57177B7098#/metadata/5aa3b739-af33-4e57-bf68-7a8757985b2d>

In addition, the glacier mass balance data are stored in the World Glacier Monitoring Service database ([dx.doi.org/10.5904/wgms-fog-2021-05](https://dx.doi.org/10.5904/wgms-fog-2021-05), WGMS, 2021), ~~dx.doi.org/10.5904/wgms-fog-2021-05~~, WGMS, 2021) and INTAROS Data Catalogue (<https://catalog-intaros.nersc.no/dataset/glacier-mass-balance-werenskioldbreen>).

All the data are also available through the Svalbard Integrated Arctic Earth Observing System (SIOS) data access portal (<https://sios-svalbard.org/metsis/search>).

Sformatowano: Czcionka: + Tekst podstawowy (Times New Roman)

Sformatowano: Czcionka: + Tekst podstawowy (Times New Roman)

Sformatowano: Czcionka: + Tekst podstawowy (Times New Roman)

Sformatowano: Czcionka: + Tekst podstawowy (Times New Roman)

Sformatowano: Czcionka: + Tekst podstawowy (Times New Roman)

Sformatowano: Czcionka: + Tekst podstawowy (Times New Roman)

Sformatowano: Normalny, Obramowanie: Góra: (Brak obramowania), Dół: (Brak obramowania), Na lewo: (Brak obramowania), Na prawo: (Brak obramowania), Pomędzy : (Brak obramowania), Tabulatory: 7,96 cm, Wyśrodkowany + 15,92 cm, Do prawej

## 89. Summary

This paper has presented details of the glaciological and meteorological dataset (2009-2020) from the Werenskioldbreen (Svalbard). The meteorological dataset includes 10 minutes, hourly and daily air temperature, relative humidity, short- and long-wave radiation, wind speed ~~and its direction~~. The glaciological dataset includes point surface mass balance (winter, summer, net), snow depth, bulk density and snow water equivalent (SWE) for the mass-balance stakes, annual glacier-wide surface mass balance (SMB) and modelled daily surface ablation. These data allow observations of the rapid changes taking place in the Arctic. In particular, they allow determining the rate of climate change directly on glaciers. Werenskioldbreen mass loss (SMB) is accelerating at a rate of -0.23 m w.e. for a decade. This is the result of air temperature increase (0.09°C per year), which is over five times faster than the global average of 0.17°C per decade (NOAA, 2020). ~~These high quality and long-term~~ observation data have been already used to assess the hydrological models and glaciological studies. The objective of releasing these data is to improve the usage of this data to calibration and validation of the remote sensing products, models as well as to increase data reuse. (Moholdt et al., 2010; Möller et al., 2011; Claremar et al., 2012; Østby et al., 2014; Błaszczyk et al., 2019).

## Acknowledgements

The study presents part of the results from the project “Hindcasting and projections of hydro-climatic conditions of Southern Spitsbergen” (grant no. 2017/27/B/ST10/01269) financed by the Polish National Science Centre and the “Arctic climate system study of ocean, sea ice, and glaciers interactions in Svalbard area”—AWAKE2 (Pol-Nor/198675/ 17/2013), supported by the National Centre for Research and Development within the Polish–Norwegian Research Cooperation Programme and the SvalGlac—Sensitivity of Svalbard glaciers to climate change, the ESF Project. Glaciological and meteorological data have been processed under assessment of the University of Silesia in Katowice data repository within the project Integrated Arctic Observing System (INTAROS). This project has received funding from the European Union's Horizon 2020 research and innovation programme under grant agreement No. 727890. A legacy from the ice2sea 7th FP and the ESF SvalGlac projects was used. The studies were carried out as part of the scientific activity of the Centre for Polar Studies (University of Silesia in Katowice) with the use of research and logistic equipment (GPR set, monitoring and measuring equipment, sensors, AWS'es, GNSS receivers, snowmobiles and other supporting equipment) of the Polar Laboratory of the University of Silesia in Katowice

The authors would like to thank the employees, doctoral students and students of the University of Silesia in Katowice for their help in the field work. We would also like to thank our colleagues from the University of Wrocław for their hospitality at the Polar Station. Stanisław Baranowski Spitsbergen and excellent cooperation. Also thanks to the members of the expedition from the Polish Polar Station Hornsund for their cooperation.

Sformatowano: Czcionka: +Tekst podstawowy (Times New Roman)

Sformatowano: Czcionka: +Tekst podstawowy (Times New Roman)

Sformatowano: Czcionka: +Tekst podstawowy (Times New Roman)

Sformatowano: Czcionka: +Tekst podstawowy (Times New Roman)

Sformatowano: Czcionka: +Tekst podstawowy (Times New Roman)

Sformatowano: Czcionka: +Tekst podstawowy (Times New Roman)

Sformatowano: Czcionka: +Tekst podstawowy (Times New Roman)

Sformatowano: Czcionka: +Tekst podstawowy (Times New Roman)

Sformatowano: Czcionka: +Tekst podstawowy (Times New Roman)

Sformatowano: Czcionka: +Tekst podstawowy (Times New Roman)

Sformatowano: Czcionka: +Tekst podstawowy (Times New Roman)

Sformatowano: Czcionka: +Tekst podstawowy (Times New Roman)

Sformatowano: Czcionka: +Tekst podstawowy (Times New Roman)

Sformatowano: Normalny, Obramowanie: Góra: (Brak obramowania), Dół: (Brak obramowania), Na lewo: (Brak obramowania), Na prawo: (Brak obramowania), Pośrodkowy : (Brak obramowania), Tabulatory: 7,96 cm, Wyśrodkowany + 15,92 cm, Do prawej

## 515 Competing interests.

The contact author has declared that neither they nor their co-authors have any competing interests

## Author Contribution

DI- Conceptualization, Formal analysis, Methodology, Validation, Writing – original draft preparation, review & editing.

MB - Investigation, Methodology, Writing – review & editing. TB - Data curation, Investigation, Writing – review & editing.

520 MG - Investigation, Methodology, Validation, Writing – review & editing. JJ – Conceptualization, Funding acquisition, Supervision, Writing – review & editing. MK - Formal analysis, Investigation, Writing – original draft preparation. ML - Investigation, Validation, Writing – review & editing. LM - Data curation, Formal analysis, Writing – original draft preparation, review & editing. LS - Investigation, Writing – review & editing.

## References

525 Baranowski, S.: Naled Ice in Front of Some Spitsbergen Glaciers, *J. Glaciol.*, 28, 211–214, <https://doi.org/https://doi.org/10.3189/S0022143000011928>, 1982.

Błaszczyk, M., Ignatiuk, D., Grabiec, M., Kolondra, L., Laska, M., Decaux, L., Jania, J., Berthier, E., Luks, B., Barzycka, B. and Czapla, M.: Quality Assessment and Glaciological Applications of Digital Elevation Models Derived from Space-Borne and Aerial Images over Two Tidewater Glaciers of Southern Spitsbergen, *Remote Sens.*, 11, 1121, <https://doi.org/10.3390/RS11091121>, 2019.

Błaszczyk, M., Jania, J. A., Ciepły, M., Grabiec, M., Ignatiuk, D., Kolondra, L., Kruss, A., Luks, B., Moskalik, M., Pastusiak, T., Strzelewicz, A., Walczowski, W. and Wawrzyniak, T.: Factors Controlling Terminus Position of Hansbreen, a Tidewater Glacier in Svalbard, *J. Geophys. Res. Earth Surf.*, 126, e2020JF005763, <https://doi.org/10.1029/2020JF005763>, 2021.

535 Błaszczyk, M., Jania, J. A. and Kolondra, L.: Fluctuations of tidewater glaciers in Hornsund Fjord (Southern Svalbard) since the beginning of the 20th century, *Polish Polar Res.*, 34, 327–352, <https://doi.org/10.2478/popore-2013-0024>, 2013.

Box, J. E., Colgan, W. T., Wouters, B., Burgess, D. O., O’Neel, S., Thomson, L. I. and Mernild, S. H.: Global sea-level contribution from Arctic land ice: 1971 to 2017, *Environ. Res. Lett.*, 13, 1–11, <https://doi.org/10.1088/1748-9326/AAAF2ED>, 2019.

540 Braithwaite, R. J.: Positive degree-day factors for ablation on the Greenland ice sheet studied by energy-balance modelling, *J. Glaciol.*, 41, 153–160, <https://doi.org/10.1017/S0022143000017846>, 1995.

Braithwaite, R. J. and Olesen, O. B.: Calculation of glacier ablation from air temperature, West Greenland, in: *Glacier fluctuations and climatic change*, edited by Oerlemans, J., Kluwer Academic Publishers, Dordrecht, 219–233, available at: [https://www.research.manchester.ac.uk/portal/en/publications/calculation-of-glacier-ablation-from-air-temperature-west-greenland\(5823a1a2-551e-4270-8d60-b5d23422ebdb\)/export.html](https://www.research.manchester.ac.uk/portal/en/publications/calculation-of-glacier-ablation-from-air-temperature-west-greenland(5823a1a2-551e-4270-8d60-b5d23422ebdb)/export.html) (last access: 23 December 2021), 1989.

- 545 [Christiansen, H.H., Gilbert, G.L., Neumann, U., Demidov, N., Guglielmin, M., Isaksen, K., Osuch, M., Boike, J.: Ground ice content, drilling methods and equipment and permafrost dynamics in Svalbard 2016–2019 \(PermaSval\). <https://doi.org/10.5281/ZENODO.4294095>, 2021.](#)
- [Claremar, B., Obleitner, F., Reijmer, C., Pohjola, V., Waxegård, A., Karner, F. and Rutgersson, A.: Applying a mesoscale atmospheric model to Svalbard glaciers, \*Adv. Meteorol.\*, 2012, doi:10.1155/2012/321649, 2012.](#)
- 550 [Cogley, J. G., Hock, R., Rasmussen, L. A., Arendt, A. A., Bauder, A., Jansson, P., Braithwaite, R. J., Kaser, G., Möller, M., Nicholson, L. and Zemp, M.: Glossary of glacier mass balance and related terms, IHP-VII Te., UNESCO-IHP, Paris, available at: <https://unesdoc.unesco.org/ark:/48223/pf0000192525> \(last access: 23 December 2021\), 2011.](#)
- [Decaux, L., Grabiec, M., Ignatiuk, D. and Jania, J.: Role of discrete water recharge from supraglacial drainage systems in modeling patterns of subglacial conduits in Svalbard glaciers, \*Cryosphere\*, 13\(3\), 735–752, doi:10.5194/TC-13-735-2019, 2019.](#)
- 555 [Førland, E. J., Isaksen, K., Lutz, J., Hanssen-Bauer, I., Schuler, T. V., Dobler, A., Gjelten, H. M., & Vikhamar-Schuler, D.: Measured and Modeled Historical Precipitation Trends for Svalbard, \*Journal of Hydrometeorology\*, 21, 1279-1296, <https://doi.org/10.1175/JHM-D-19-0252.1>, 2020.](#)
- [Gabbi, J., Carenzo, M., Pellicciotti, F., Bauder, A. and Funk, M.: A comparison of empirical and physically based glacier surface melt models for long-term simulations of glacier response, \*J. Glaciol.\*, 60\(224\), 1140–1154, doi:10.3189/2014JOG14J011, 2014.](#)
- 560 [Grabiec, M., Ignatiuk, D., Jania, J. A., Moskalik, M., Głowacki, P., Błaszczuk, M., Budzik, T. and Walczowski, W.: Coast formation in an Arctic area due to glacier surge and retreat: The Hornbreen–Hambergbreen case from Spistbergen, \*Earth Surf. Process. Landforms\*, 43, 387–400, <https://doi.org/10.1002/ESP.4251>, 2018.](#)
- 565 [Grabiec, M., Budzik, T. and Głowacki, P.: Modeling and Hindcasting of the Mass Balance of Werenskioldbreen \(Southern Svalbard\), 44, 164–179, <https://doi.org/10.1657/1938-4246-44.2.164>, 2018, 2018, 2012.](#)
- [Gwizdała, M., Jeleńska, M. and Łęczyński, L.: The magnetic method as a tool to investigate the Werenskioldbreen environment \(south-west Spitsbergen, Arctic Norway\), \*Polar Res.\*, 37, 1–9, <https://doi.org/10.1080/17518369.2018.1436846>, 2018.](#)
- [Hagen, J., Dunse, T., Eiken, T., Kohler, J., Moholdt, G., Nuth, C., Schuler, T. and Østby, T.: The mass balance of the Austfonna Ice Cap, Svalbard, 2004–2010, \*Geophys. Res. Abstr.\* 14, EGU2012-6085-1, 2012.](#)
- 570 [Hanssen-Bauer, I., Førland, E.J., Hisdal, H., Mayer, S., Sandø, A.B. and Sorteberg, A. \(Eds.\): Climate in Svalbard 2100 - a knowledge base for climate adaptation, Norway, Norwegian Centre of Climate Services \(NCCS\) for Norwegian Environment Agency \(Miljødirektoratet\), 208pp, \(NCCS report 1/2019\), <https://doi.org/10.25607/OBP-888>, 2019.](#)
- [Hamed, K. H. and Rao, R.: A modified Mann-Kendall trend test for autocorrelated data, \*J. Hydrol.\*, 204, 182–196, 1998.](#)
- 575 [Ignatiuk, D.: Meteorological data from the Werenskioldbreen \(Svalbard\) 2009–2020 \[Data set\]. Zenodo. <https://doi.org/10.5281/zenodo.5791748><https://doi.org/10.5281/zenodo.5791748>, 2021a.](#)

**Sformatowano:** Czcionka: +Tekst podstawowy (Times New Roman)

**Sformatowano:** Czcionka: +Tekst podstawowy (Times New Roman)

**Sformatowano:** Czcionka: +Tekst podstawowy (Times New Roman)

**Sformatowano:** Czcionka: +Tekst podstawowy (Times New Roman)

**Sformatowano:** Czcionka: +Tekst podstawowy (Times New Roman)

**Sformatowano:** Czcionka: +Tekst podstawowy (Times New Roman)

**Sformatowano:** Normalny, Obramowanie: Góra: (Brak obramowania), Dół: (Brak obramowania), Na lewo: (Brak obramowania), Na prawo: (Brak obramowania), Pośrodku: (Brak obramowania), Tabulatory: 7,96 cm, Wyśrodkowany + 15,92 cm, Do prawej

Ignatiuk, D.: Glaciological data (point mass balance, SWE, snow depth, bulk snow density, modelled runoff) from Werenskioldbreen (Svabard) 2009-2020 [Data set]. Zenodo. <https://doi.org/10.5281/zenodo.5792168><https://doi.org/10.5281/zenodo.5792168>, 2021b.

580 Ignatiuk, D., Piechota, A., Ciepły, M. and Luks, B.: Changes of altitudinal zones of Werenskioldbreen and Hansbreen in period 1990 – 2008, Svalbard, AIP Conf. Proc., 1618, 280, <https://doi.org/10.1063/1.4897727>, 2015.

IPCC: The Ocean and Cryosphere in a Changing Climate 2019, <https://www.ipcc.ch/srocc/home/>, last access: 1 April 2020.

Hock, R.: Temperature index melt modelling in mountain areas, J. Hydrol., 282, 104–115, [https://doi.org/10.1016/S0022-1694\(03\)00257-9](https://doi.org/10.1016/S0022-1694(03)00257-9), 2003.

585 Isaksen, K., Nordli, Førland, E. J., Łupikasza, E., Eastwood, S. and Niedźwiedź, T.: Recent warming on Spitsbergen—Influence of atmospheric circulation and sea ice cover, J. Geophys. Res. Atmos., 121, 11913–11931, <https://doi.org/10.1002/2016JD025606>, 2016.

Jania, J., Majchrowska, E., Ignatiuk, D., Marszałek, H. and Wąsik, M.: Seasonal and interannual variability in runoff from the Werenskioldbreen catchment, Spitsbergen, Polish Polar Res., 36, 197–224, <https://doi.org/10.1515/popore-2015-0014>, 2015.

590 Łepkowska, E. and Stachnik, L.: Which Drivers Control the Suspended Sediment Flux in a High Arctic Glacierized Basin (Werenskioldbreen, Spitsbergen)?, Water, 10, 1408, <https://doi.org/10.3390/W10101408>, 2018.

Łupikasza, E. B., Ignatiuk, D., Grabiec, M., Cielecka-Nowak, K., Laska, M., Jania, J., Luks, B., Uszczyk, A. and Budzik, T.: The Role of Winter Rain in the Glacial System on Svalbard, Water, 11, 334, <https://doi.org/10.3390/W11020334>, 2019.

Majchrowska, E., Ignatiuk, D., Jania, J., Marszałek, H. and Wasik, M.: Seasonal and interannual variability in runoff from the Werenskioldbreen catchment, Spitsbergen, Polish Polar Res., 36, 197–224, <https://doi.org/10.1515/popore-2015-0014>, 2015.

595 ~~NOAA: National Centers for Environmental Information, Climate at a Glance, Global Time Series, available at: <https://www.ncei.noaa.gov/eag/>, last access: 23 October 2021.~~

~~Moholdt, G., Nuth, C., Hagen, J. O. and Kohler, J.: Recent elevation changes of Svalbard glaciers derived from ICESat laser altimetry, Remote Sens. Environ., 114(11), 2756–2767, doi:10.1016/J.RSE.2010.06.008, 2010.~~

600 ~~Möller, M., Finkelnburg, R., Braun, M., Hock, R., Jonsell, U., Pohjola, V. A., Scherer, D. and Schneider, C.: Climatic mass balance of the ice cap Vestfonna, Svalbard: A spatially distributed assessment using ERA-Interim and MODIS data, J. Geophys. Res. Earth Surf., 116(F3), 3009, doi:10.1029/2010JF001905, 2011.~~

605 ~~Noël, B., Jakobs, C. L., van Pelt, W. J. J., Lhermitte, S., Wouters, B., Kohler, J., Hagen, J. O., Luks, B., Reijmer, C. H., van de Berg, W. J. and van den Broeke, M. R.: Low elevation of Svalbard glaciers drives high mass loss variability, Nat. Commun., 11, 4597, <https://doi.org/10.1038/s41467-020-18356-1>, 2020.~~

Nordli, Ø., Przybylak, R., Ogilvie, A. E. J. and Isaksen, K.: Long-term temperature trends and variability on spitsbergen: The extended svalbard airport temperature series, 1898-2012, Polar Res., 33, 1898–2012, [https://doi.org/10.3402/POLAR.V33.21349/SUPPL\\_FILE/ZPOR\\_A\\_11818879\\_SM0001.PDF](https://doi.org/10.3402/POLAR.V33.21349/SUPPL_FILE/ZPOR_A_11818879_SM0001.PDF), 2014.

Sformatowano: Czcionka: +Tekst podstawowy (Times New Roman)

Sformatowano: Czcionka: +Tekst podstawowy (Times New Roman)

Sformatowano: Normalny, Obramowanie: Góra: (Brak obramowania), Dół: (Brak obramowania), Na lewo: (Brak obramowania), Na prawo: (Brak obramowania), Pośrodku: (Brak obramowania), Tabulatory: 7,96 cm, Wyśrodkowany + 15,92 cm, Do prawej



610 Nuth, C., Gilbert, A., Köhler, A., McNabb, R., Schellenberger, T., Sevestre, H., Weidle, C., Girod, L., Luckman, A. and Kääh, A.: Dynamic vulnerability revealed in the collapse of an Arctic tidewater glacier, *Sci. Reports* 9, 5541, <https://doi.org/10.1038/s41598-019-41117-0>, 2019.

Ohmura, A.: Physical basis for the temperature-based melt-index method, *J. Appl. Meteorol.*, 40, 753–761, [https://doi.org/10.1175/1520-0450\(2001\)040<0753:PBFTTB>2.0.CO;2](https://doi.org/10.1175/1520-0450(2001)040<0753:PBFTTB>2.0.CO;2), 2001.

615 Osuch, M. and Wawrzyniak, T.: Inter- and intra-annual changes in air temperature and precipitation in western Spitsbergen, *Int. J. Climatol.*, 37, 3082–3097, <https://doi.org/10.1002/JOC.4901>, 2017.

Pälli, A., Osuch, M., Wawrzyniak, T. and Lepkowska, E.: Changes in the flow regime of High Arctic catchments with different stages of glaciation, SW Spitsbergen, *Sci. Total Environ.*, 817, 152924, doi:10.1016/J.SCITOTENV.2022.152924, 2022.

Østby, T. I., Schuler, T. V. and Westermann, S.: Severe cloud contamination of MODIS Land Surface Temperatures over an Arctic ice cap, *Svalbard, Remote Sens. Environ.*, 142, 95–102, doi:10.1016/J.RSE.2013.11.005, 2014.

620 Østby, T. I., Schuler, T. V., Ove Hagen, J., Hock, R., Kohler, J. and Reijmer, C. H.: Diagnosing the decline in climatic mass balance of glaciers in Svalbard over 1957-2014, *Cryosphere*, 11(1), 191–215, doi:10.5194/TC-11-191-2017, 2017.Pälli, A., Moore, J. C., Jania, J., Kolondra, L. and Glowacki, P.: The drainage pattern of Hansbreen and Werenskiöldbreen, two polythermal glaciers in Svalbard, *Polar Res.*, 22, 355–371, <https://doi.org/10.1111/j.1751-8369.2003.tb00117.x>, 2003.

625 Pellicciotti, F., Ragetti, S., Carenzo, M. and McPhee, J.: Changes of glaciers in the Andes of Chile and priorities for future work, *Sci. Total Environ.*, 493, 1197–1210, doi:10.1016/J.SCITOTENV.2013.10.055, 2014.

Schuler, T. V., Dunse, T., Østby, T. I. and Hagen, J. O.: Meteorological conditions on an Arctic ice cap—8 years of automatic weather station data from Austfonna, Svalbard, *Int. J. Climatol.*, 34, 2047-2058, 2014, <https://doi.org/10.1002/joc.3821>.

630 Schuler, T. V., Kohler, J., Elagina, N., Hagen, J. O. M., Hodson, A. J., Jania, J. A., Kääh, A. M., Luks, B., Małecki, J., Moholdt, G., Pohjola, V. A., Sobota, I. and Van Pelt, W. J. J.: Reconciling Svalbard Glacier Mass Balance, *Front. Earth Sci.*, 8, 156, <https://doi.org/10.3389/FEART.2020.00156/BIBTEX>, 2020.

Sen, P. K.: Estimates of the regression coefficient based on Kendall's tau, *J. Am. Stat. Assoc.*, 63, 1379–1389, <https://doi.org/10.2307/2285891>, 1968.

635 Stachnik, L., Majchrowska, E., Yde, J. C., Nawrot, A. P., Cichała-Kamrowska, K., Ignatiuk, D. and Piechota, A.: Chemical denudation and the role of sulfide oxidation at Werenskiöldbreen, Svalbard, *J. Hydrol.*, 538, 177–193, <https://doi.org/10.1016/J.JHYDROL.2016.03.059>, 2016a.

Stachnik, L., Yde, J. C., Kondracka, M., Ignatiuk, D. and Grzesik, M.: Glacier naled evolution and relation to the subglacial drainage system based on water chemistry and GPR surveys (Werenskiöldbreen, SW Svalbard), *Ann. Glaciol.*, 57, 19–30, <https://doi.org/10.1017/AOG.2016.9>, 2016b.

640 Stachnik, L., Yde, J. C., Nawrot, A., Uzarowicz, L., Lepkowska, E. and Kozak, K.: Aluminium in glacial meltwater demonstrates an association with nutrient export (Werenskiöldbreen, Svalbard), *Hydrol. Process.*, 33, 1638–1657, <https://doi.org/10.1002/HYP.13426>, 2019.

Sformatowano: Czcionka: +Tekst podstawowy (Times New Roman)

Sformatowano: Czcionka: +Tekst podstawowy (Times New Roman)

Sformatowano: Czcionka: +Tekst podstawowy (Times New Roman)

Sformatowano: Normalny, Obramowanie: Góra: (Brak obramowania), Dół: (Brak obramowania), Na lewo: (Brak obramowania), Na prawo: (Brak obramowania), Pośrodku: (Brak obramowania), Tabulatory: 7,96 cm, Wyśrodkowany + 15,92 cm, Do prawej

Sturm, M., Taras, B., Liston, G. E., Derksen, C., Jonas, T. and Lea, J. <https://doi.org/10.1175/2010JHM1202.1>, 2010.: Estimating Snow Water Equivalent Using Snow Depth Data and Climate Classes, *J. Hydrometeorol.*, 11, 1380–1394, <https://doi.org/10.1175/2010JHM1202.1>, 2010.

Sformatowano: Czcionka: +Tekst podstawowy (Times New Roman)

645 Sułowicz, S., Bondarczuk, K., Ignatiuk, D., Jania, J. A. and Piotrowska-Seget, Z.: Microbial communities from subglacial water of naled ice bodies in the forefield of Werenskioldbreen, Svalbard, *Sci. Total Environ.*, 723, 138025, <https://doi.org/10.1016/J.SCITOTENV.2020.138025>, 2020.

Sformatowano: Czcionka: +Tekst podstawowy (Times New Roman)

650 Uszczyk, A., Grabiec, M., Laska, M., Kuhn, M. and Ignatiuk, D.: Importance of snow as component of surface mass balance of Arctic glacier (Hansbreen, southern Spitsbergen), *Polish Polar Res.*, 40, 311–338, <https://doi.org/10.24425/PPR.2019.130901>, 2019.

Van Pelt, W., Pohjola, V., Pettersson, R., Marchenko, S., Kohler, J., Luks, B., Ove Hagen, J., Schuler, T. V., Dunse, T., Noël, B. and Reijmer, C.: A long-term dataset of climatic mass balance, snow conditions, and runoff in Svalbard (1957–2018), *Cryosphere*, 13, 2259–2280, <https://doi.org/10.5194/TC-13-2259-2019>, 2019.

655 [Vikhamar-Schuler, D., Isaksen, K., Haugen, J. E., Tømmervik, H., Luks, B., Schuler, T. V. and Bjerke, J. W.: Changes in Winter Warming Events in the Nordic Arctic Region, \*Journal of Climate\*, 29, 6223–6244, <https://doi.org/10.1175/JCLI-D-15-0763.1>, 2016.](https://doi.org/10.1175/JCLI-D-15-0763.1)

660 [Walcowski, W., Beszczynska-Möller, A., Wieczorek, P., Merchel, M. and Grynzel, A.: Oceanographic observations in the Nordic Sea and Fram Strait in 2016 under the IO PAN long-term monitoring program AREX, \*Oceanologia\*, 59, 187–194, <https://doi.org/10.1016/J.OCEANO.2016.12.003>, 2017.](https://doi.org/10.1016/J.OCEANO.2016.12.003)

Sformatowano: Czcionka: +Tekst podstawowy (Times New Roman)

665 Wawrzyniak, T. and Osuch, M.: A 40-year High Arctic climatological dataset of the Polish Polar Station Hornsund (SW Spitsbergen, Svalbard), *Earth Syst. Sci. Data*, 12, 805–815, <https://doi.org/10.5194/ESSD-12-805-2020>, 2020.

Wawrzyniak, T., Osuch, M., Napiórkowski, J. and Westermann, S.: Modelling of the thermal regime of permafrost during 1990–2014 in Hornsund, Svalbard, *Polish Polar Res.*, 37, 219–242, <https://doi.org/10.1515/POPORE-2016-0013>, 2016.

665 WGMS: Fluctuations of Glaciers Database. World Glacier Monitoring Service, Zurich, Switzerland. DOI:10.5904/wgms-fog-2021-05, 2021.

[Yadav, J., Kumar, A. and Mohan, R.: Dramatic decline of Arctic sea ice linked to global warming, \*Nat. Hazards\*, 103\(2\), 2617–2621, \[doi:10.1007/S11069-020-04064-Y\]\(https://doi.org/10.1007/S11069-020-04064-Y\), 2020.](https://doi.org/10.1007/S11069-020-04064-Y)

Sformatowano: Czcionka: +Tekst podstawowy (Times New Roman)

Sformatowano: Normalny, Obramowanie: Góra: (Brak obramowania), Dół: (Brak obramowania), Na lewo: (Brak obramowania), Na prawo: (Brak obramowania), Pomiedzy : (Brak obramowania), Tabulatory: 7,96 cm, Wyśrodkowany + 15,92 cm, Do prawej